β-bursts over frontal cortex track the surprise of unexpected events in auditory, visual, and tactile modalities

Joshua R. Tatz,[1,2,3] Alec Mather,[1] & Jan R. Wessel[1,2,3]

[1]Department of Psychological and Brain Sciences, University of Iowa, Iowa, USA

[2]Department of Neurology, University of Iowa Hospital and Clinics, Iowa City, Iowa, USA

[3]Cognitive Control Collaborative University of Iowa, Iowa, USA

Address Correspondence to

Joshua R. Tatz

Department of Psychological and Brain Sciences

University of Iowa

Iowa City, IA, 52242

Joshua-tatz@uiowa.edu

Abstract

One of the fundamental ways in which the brain regulates and monitors behavior is by making predictions about the sensory environment and adjusting behavior when those expectations are violated. As such, surprise is one of the fundamental computations performed by the human brain. In recent years, it has been well-established that one key aspect by which behavior is adjusted during surprise is inhibitory control of the motor system. Moreover, since surprise automatically triggers inhibitory control without much proactive influence, it can provide unique insights into largely reactive control processes. Recent years have seen tremendous interest in burst-like β frequency events in the human (and non-human) local field potential – especially over (pre)frontal cortex) – as a potential signature of inhibitory control. To date, β bursts have only been studied in paradigms involving a substantial amount of proactive control (such as the stop-signal task). Here, we used two cross-modal oddball tasks to investigate whether surprise processing is accompanied by increases in scalp-recorded β-bursts. Indeed, we found that unexpected events in all tested sensory domains (haptic, auditory, visual) were followed by low-latency increases in β-bursting over frontal cortex. Moreover, across experiments, β-burst rates were positively correlated with estimates of surprise derived from Shannon's information theory. As such, the current work clearly implicates frontal β bursts as a signature of surprise processing. We discuss these findings in the context of common frameworks of inhibitory and cognitive control after unexpected events.

Keywords: Shannon surprise, Bayesian surprise, oddball, reactive inhibitory control; beta bursts

INTRODUCTION

Throughout the day, we constantly encounter external information translated by our various senses. While navigating this diverse sensory environment, our brain steadily generates predictions about this incoming stream of crossmodal information (Egner et al., 2010; Phillips et al., 2016). One of the key roles of frontal cortex is to detect deviations from such sensory predictions (Corbetta & Shulman, 2002; Kim, 2014). Indeed, identifying and modifying behavior according to unexpected perceptual events can have profound consequences on our lives. For instance, seeing a predator, hearing a roar, or feeling something crawl on one's skin are all unexpected events that require rapid behavioral and cognitive adjustments. Subsequently, unexpected events provide a useful backdrop with which to explore the processes underlying adaptive behavior.

Indeed, unexpected perceptual events trigger multiple well-established cognitive and motor processes. Friston's (2010) influential free-energy principle suggests that descending neural volleys convey predictions about the sensory environment, whereas ascending volleys convey violations of these expectancies, or prediction error. Some work has used simple mathematical models (Shannon, 1948; Baldi & Itti, 2010) to quantify surprise at the single-trial level, thereby showing that various neural signals may reflect such straightforward computations (e.g., Mars et al., 2008; O'Reilly et al., 2013; Nassar et al., 2019; Wessel & Huber, 2019). In addition to surprise processing, unexpected events are thought to capture attention in a bottom-up fashion and may interrupt goal-directed attentional representations, as in Corbetta and Shulman's (2002) "circuit breaker" model of attention. Along these lines, target detection ability (e.g., Asplund et al., 2010), attentional representations indexed by steady-state visual evoked potential (e.g., Soh & Wessel, 2021), and content in active working memory may all be impaired by unexpected events (e.g.,

Wessel, 2018a; Hakim et al., 2021). Likewise, unexpected events prompt inhibition and disrupt ongoing action. Task-irrelevant unexpected events can induce reaction time slowing (e.g., Parmentier et al., 2008) as well as disrupt repetitive finger tapping (Horstmann, 2015) or the maintenance of isometric force contractions (Novembre et al., 2018). In addition, numerous studies using TMS to measure cortico-motor excitability have found a broad physiological suppression of the cortico-motor system after unexpected events, including at entirely task-irrelevant muscles (Wessel & Aron, 2013; Dutra et al., 2018; Iacullo et al., 2020; Tatz et al., 2021).

Further underscoring the link between surprise and inhibitory control, unexpected events and action cancellation are accompanied by common neurophysiological signatures. As the gold-standard method of testing action cancellation, the stop-signal task (SST) is the primary tool used to study motor inhibition (Verbruggen et al., 2019). In the SST, prepotent responses to Go signals must be inhibited upon interruption by an infrequent Stop signal. One common signature that is observed both after such stop-signals and after unexpected events outside of stop-signal paradigms is the above-mentioned suppression of the motor system (Badry et al., 2009; Cai et al., 2012; Wessel et al., 2013; Tatz et al., 2021). Another common signature is the fronto-central (FC) P3 event-related potential. The FC P3 ERP accompanies unexpected events and stop signals and is likely generated by the same underlying neural generator (Dutra et al., 2018; Wessel & Huber, 2019). Furthermore, regions in frontal cortex that are reliably active during successful response inhibition are likewise active following unexpected events in oddball or Posner cueing tasks (e.g., Levy & Wagner, 2011). Together, these findings suggest common neural processes that are active during both surprise and action cancellation.

A missing link in this picture concerns β-bursts, which have attracted considerable recent attention as a newly discovered inhibitory signature in the local field potential. β-bursts are

transient, non-linear activity increases in β band activity (15-29 Hz) that occur in both cortical and subcortical regions of the brain (Feingold et al., 2015; Tinkhauser et al., 2018, Diesburg et al., 2021). β-bursts have been shown to represent time-frequency dynamics at the single-trial level more accurately and better predict behavior than average β power (Shin et al., 2017; Little et al., 2019; Wessel, 2020) and are potentially generated by a straightforward biophysical mechanism that maps onto inhibitory and excitatory thalamocortical dynamics (Sherman et al., 2016).

In line with their purported role in reflecting inhibitory neural processes, several studies have recently linked β-bursts to action cancellation and / or motor inhibition more generally. Little et al. (2019) showed that sensorimotor β-bursts that occurred close to movement increased RT. Wessel (2020) demonstrated that healthy adults exhibit decreased bilateral sensorimotor β-bursts in the moments leading up to motor execution along with further decreases in contralateral sites just before movement. The same study and subsequent work have identified relationships between β-bursts at more frontal sites and action cancellation. Wessel (2020) found that successful stop trials were characterized by an increase in frontocentral β-bursts which in turn prompted increased β-bursting at the bilateral sensorimotor sites. Jana et al. (2020) similarly observed an increase in frontal β-bursts on successful stop trials and found that their latency correlated with the latency of the downturn of subthreshold electromyographic activity evoked on a portion of successful stop trials. Because these increases in β-bursts occurred at around 120 ms following the stop signal and even earlier than when they first observed global motor suppression using TMS (~140 ms), Jana et al. (2020) suggested that these β-bursts may trigger the stop process. Diesburg et al. (2021) identified β-burst increases in local field potential recordings from subthalamic nucleus (STN) and motor thalamus on successful stop trials and further showed that these subcortical β-burst were associated with subsequent, low-latency sensorimotor β-bursts. Tinkhauser et al. (2018) found

resting state phase coupling between STN and motor cortex that was augmented during β-bursts. This suggests β-bursts may provide a vehicle of long-range communication. Finally, β-bursts have been linked to pathophysiology of disease (Anidi et al., 2018; Lofredi et al., 2019; Pina-Fuentes et al., 2019), and clinical procedures aimed at targeting STN β-bursts in individuals with Parkinson's Disease have shown promise in alleviating motor symptoms (Tinkhauser, Pogosyan, Little, et al., 2017; Tinkhauser, Pogosyan, Tan, et al., 2017).

Given the above-mentioned tight link between surprise and inhibition, and given the tight relationship between the novel β-burst signature and inhibitory control, one straightforward hypothesis is that β-bursts should be increased after unexpected events. Such a demonstration would be important for establishing a role of β-bursts in reactive inhibitory control. By reactive inhibitory control, we mean inhibition that is triggered by a stimulus rather than its anticipation (Aron, 2011). In the SST, the stop signal occurs on only a fraction of trials and uncertainty surrounds when it will occur. Consequently, some reactive inhibitory control is likely triggered by the stop signal. However, participants are not only aware that the stop signal will occur but are explicitly monitoring for it. Consequently, in the SST, reactive inhibitory control processes are necessarily conflated with proactive inhibitory control, or adjustments made in anticipation of the expected stop signal (Aron, 2011). Unexpected events therefore offer a cleaner window into purely reactive control and one that is better aligned with how inhibition transpires in our day to day (Wessel, 2018a). That is, outside of the laboratory we seldom make advanced preparations for a particular unexpected event but instead decide how to react after its occurrence (e.g., holding still after feeling something crawl across one's skin).

The primary goal of the current study is to investigate whether frontal β-bursts are elevated following unexpected events. To this end, we use two datasets. In the first dataset, participants

completed a trimodal cross-modal oddball task in which unexpected events could occur randomly and without warning in auditory, visual, and haptic modalities. In the second dataset, participants completed a bimodal cross-modal oddball task in which unexpected events occurred in either the auditory or visual modalities. This second dataset was previously reported by Wessel and Huber (2019) but is here newly analyzed for β-bursts. Regarding the first dataset, we hypothesized that FC β-bursts would be increased in all three modalities. We then further explored the relationship of these β-bursts to surprise model estimates and RT at the single-trial level. To this end, we use our second dataset (from Wessel & Huber, 2019) to independently verify our exploratory findings in this regard that were generated from the first (newly collected) dataset.

METHOD

Participants. Dataset 1 includes 40 healthy young adult volunteers (21 female; 5 left-handed; $M_{\text{Age}} = 21.35$, $SD = 4.17$, range = 18 to 40). Data from three additional participants were excluded (two because of technical error in the CMO task and one who was unable to complete the CMO task). Dataset 2 includes the 55 healthy young adults from Wessel and Huber (2019). Participants in both datasets were recruited from the Iowa City community and from among University of Iowa students seeking research credit for psychology classes. Participants were compensated with course credit or at a rate of $15/hour. Both experiments were approved by the local institutional review board (#201511709).

Previous work on β-bursts from our group has shown that, in the stop-signal task (SST), increased FC β-bursts for successful stop compared to matched go trials show a large effect size ($dz = .8$). Subsequently, as few as 23 participants would be sufficient to attain 95% power for

detecting an effect of equal size at an alpha level of .05. However, greater power is often required to establish reliable brain-behavior relationships. Prior work from our group on proactive β-bursts evinced such relationships with a sample of 41 participants (Soh et al., 2021). We therefore targeted a similar sample size in Dataset 1. Prior to experimentation, piloting was performed to ensure that none of the unexpected events induced startle responses.

Materials. The methods used in Dataset 1 are the same as in Dataset 2 except where otherwise noted. The methods reported here are adapted from Wessel and Huber (2019). Stimuli for both experiments were delivered using Psychophysics toolbox 3 (Brainard, 1997) on MATLAB 2015 (TheMathWorks, Natick, MA) on an IBM-compatible computer running Fedora Linux. Visual stimuli were presented on an ASUS VG278Q low-latency flat screen monitor (144 Hz), and auditory stimuli were played at conversational levels (~70 dB SPL) through speakers positioned on either side of the monitor. Tactile stimuli were delivered over custom-built response devices (Engineering Electronics Shop, University of Iowa, Iowa City, IA) that interfaced with a Psychtoolbox compatible data acquisition device (UBS-1208FS, Measurement Computing Corporation, Norton, MA) to record button presses from the thumb and vibrate motors at rates of 8300 RPM. The response/vibration device were only used in Dataset 1. In Dataset 2 (and during the SST functional localizer task for participants in Dataset 1), participants made responses with each index finger on a QWERTY keyboard.

Procedure. A diagram of the cross-modal oddball (CMO) tasks used in each dataset can be found in Fig. 1. In Dataset 1, each trial, started with a white fixation cross centered on a black background that was displayed for 500 ms. This was followed by the cue which was displayed for

200 ms. On 80% of trials, the cue was a standard event consisting of a green circle and a 600-Hz sine wave tone. On the remaining 20% of trials, 6.7% of trials featured unexpected visual events, 6.7% featured unexpected auditory events, and 6.7% featured unexpected haptic events. Thus, the unexpected events could occur in any (but not multiple) sensory domain(s). On visually unexpected trials, the green circle of the standard event was replaced by one of seven shapes (upwards triangle, downwards triangle, square, diamond, cross, hexagon, or serifed "I" shape) and one of 15 non-green colors equally spaced across the RGB spectrum. Thus, visually unexpected events were also unique, or novel. Likewise, on auditory unexpected trials, the tone was replaced by a novel birdsong that matched the tone in amplitude. On unexpected haptic trials, the response devices that participants held in either hand vibrated bilaterally. The participants were instructed in advance about the properties of the standard event and that it was important to pay attention to this cue because it always took the same amount of time before the target would appear after the cue. Following presentation of the cue, the fixation was displayed for 300 ms prior to the presentation of the imperative stimuli. Thus, there was always a fixed delay of 500 ms before target onset. Participants had to respond within 1000 ms following the presentation of the target. After the response deadline, a variable inter-trial interval of 2600 to 3100 took place (in 100 ms steps, sampled from a uniform distribution) to preclude anticipation of the onset of the cue in the subsequent trial. Before beginning the formal experiment participants completed 10 practice trials with no unexpected events. They then completed 240 trials in the main experiment which were divided into 4 blocks of 60 trials with self-paced breaks in between.

The CMO task used in Dataset 2 was identical to Dataset 1 with two exceptions: In Dataset 2, 10% of trials featured unexpected auditory events and 10% featured unexpected visual events

(thus, the overall frequency of the standard and unexpected events was kept the same across datasets 80/20%). Participants also responded by pressing keys with their index fingers.

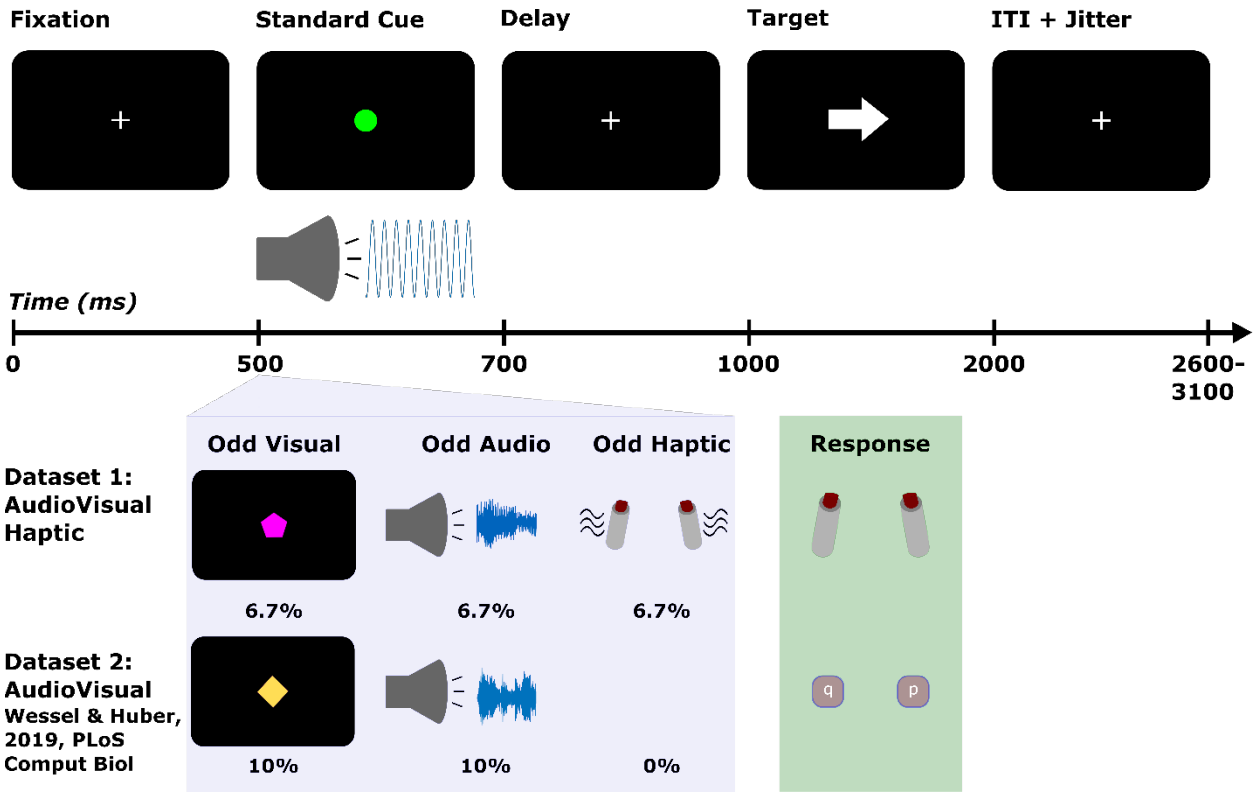

Fig. 1 Task diagrams for the cross-modal oddball tasks in Datasets 1 and 2. *The top row shows the timing and the display on standard cue trials (which were the same in both datasets). The standard cue consisted of a green circle and a 600 Hz pure tone. On trials with unexpected events, these were replaced by visual (unique shape/colors) or auditory novels (birdsong) or in the case of unexpected haptic events (in Dataset 1) the response devices participants held additionally vibrated. The light purple box illustrates examples of the unexpected events as well as their respective probabilities. The light green box depicts response devices (for Dataset 1, bilateral thumb presses, and for Dataset 2, bilateral index keypresses on a QWERTY keyboard).*

Following the CMO task, participants in both datasets completed the SST as a functional localizer task. As in Dataset 2, participants completed a standard visual SST consisting of 300 trials completed in six, 50 trial blocks. The stop-signal probability was .33 resulting in 200 go trials and 100 stop trials. The trial began with a black fixation cross presented for 500 ms on gray background. After this, the left or right-pointing arrows (in black) were presented as the go signal. On go trials, participants pressed "z" key on a QWERTY keyboard in response to left arrows and the "m" key in response to right arrows. On stop trials, the arrow turned red after the stop-signal delay (SSD) and participants were instructed to try their best to cancel their response while still responding as quickly and accurately as possible to the go signals. The SSD was initialized to 200 ms (separately for each hand) and increased in 50 ms increments following successful stop trials and decreased in 50 ms following failed stop trials. Trial duration was fixed at 3000 ms. Participants completed 24 practice (8 stop-signal) trials before the formal SST experiment began. One person followed instructions to respond as quickly as possible for the CMO task but did not do so for the SST (as evidenced by SSDs of 1000 ms indicating extreme waiting for the stop signal and nullifying the ability of the task to measure action cancellation). Data from this individual were only excluded from analyses involving the SST data.

EEG recording. Scalp-surface EEG was acquired from a 62-channel passive electrode cap connected to BrainVision MRplus amplifiers (BrainProducts, Garching, Germany). Additional electrodes were placed over the left canthus of the left eye and beneath the left eye (on the orbital bone). The ground electrode was located at the Fz electrode position, and the reference electrode was placed at the Pz electrode. EEG was digitized at a sampling rate of 500 Hz.

EEG preprocessing. Preprocessing was performed as described in Wessel and Huber (2019). We used custom MATLAB (MATLAB 2015b, TheMathWorks) functions using the EEGLAB toolbox (Delorme & Makeig, 2004). The imported data were filtered with symmetric two-way least squares finite impulse response filters (high-pass cutoff: .3 Hz, low-pass cutoff: 30Hz). Outlier statistics were used to automatically reject non-stereotyped artifacts (joint probability and joint kurtosis with cutoffs set to 5 SD, cf., Delorme et al., 2007). The data were re-referenced to the common average and subjected to temporal infomax independent component analysis (ICA) decomposition (Bell & Sejnowski, 1995) with extension to sub-Gaussian sources (Lee et al., 1999). Among the resulting components, those corresponding to eye-movement and electrode artifacts were removed from the data based on outlier statistics and non-dipolar components with a residual variance cutoff of 15% (Delorme et al., 2012).

Behavioral analysis. The RT data were initially submitted to a Bayesian repeated-measures (RM)-ANOVA with the factors Event type (Standard, Unexpected audio, Unexpected haptic, and Unexpected visual) and Block (1, 2, 3, and 4) as within-subject factors. Moreover, as planned comparisons, Bayesian paired *t*-tests were used to compare RTs following each type of unexpected event to those following the standard event within each block (for a total of 12 comparisons). Error rate and miss rate were similarly analyzed with Bayesian RM-ANOVAs and Bayesian paired-tests. For these analyses and subsequent Bayesian tests, the data were analyzed using JASP 0.15.0.0 (Love et al., 2019) after exporting the data from MATLAB. Throughout, Bayes Factors (BF) are framed as evidence favoring the alternative hypothesis (H1) or the null hypothesis (H0) with $BF \sim 1$ corresponding to inconclusive, $BF > 1$ corresponding to anecdotal

evidence, $BF > 3$ corresponding to moderate evidence, and $BF > 10$ corresponding to strong evidence. For all tests, non-informative (or "empirical") priors are used.

The subsequent SST functional localizer task was examined in terms of the mean Go-trial RT, mean failed-stop RT, and mean stop-signal RT (estimated via the integration method, Verbruggen & Logan, 2009; Boehler et al., 2014).

Modeling surprise at the single-trial level. There is some debate in the literature regarding the appropriate mathematical quantification of surprise (e.g., Shannon, 1948; Baldi & Itti, 2010; O'Reilly et al., 2013).

Based on Shannon's theory of information, surprise is given by the following equation:

$$Shannon\ Surprise_i = -log\left(p_{unexpected_cue}(1 \ldots i-1)\right) \quad (1)$$

This equation quantifies the unexpectedness of the *i*th trial by taking the log inverse of the prior probability of the unexpected event. Since -log(0) is undefined, the surprise value for the first unexpected event (for which the prior is 0) was here defaulted to the next largest integer above the surprise value of the second unexpected event. Fig. 2 provides an example of the Shannon surprise values from one participant from Dataset 1.

In contrast, Bayesian surprise (Baldi & Itti, 2010), an alternative quantification, uses the Kullback-Leibler divergence, and is given by the following equation:

$$Bayesian\ Surprise_i = log_2\left(\frac{p_{unexpected_cue}(1 \ldots i)}{p_{unexpected_cue}(1 \ldots i-1)}\right) \quad (2)$$

Bayesian surprise captures the difference between the prior (denominator) and posterior probabilities of an event (numerator). For this reason, some have argued that Bayesian surprise should be more accurately termed 'model updating' or 'learning' (e.g., O'Reilly et al., 2013; Nassar et al., 2019). Here, the first surprising value following the first unexpected event was defaulted to 1 because -log(0) (and division by zero) is undefined.

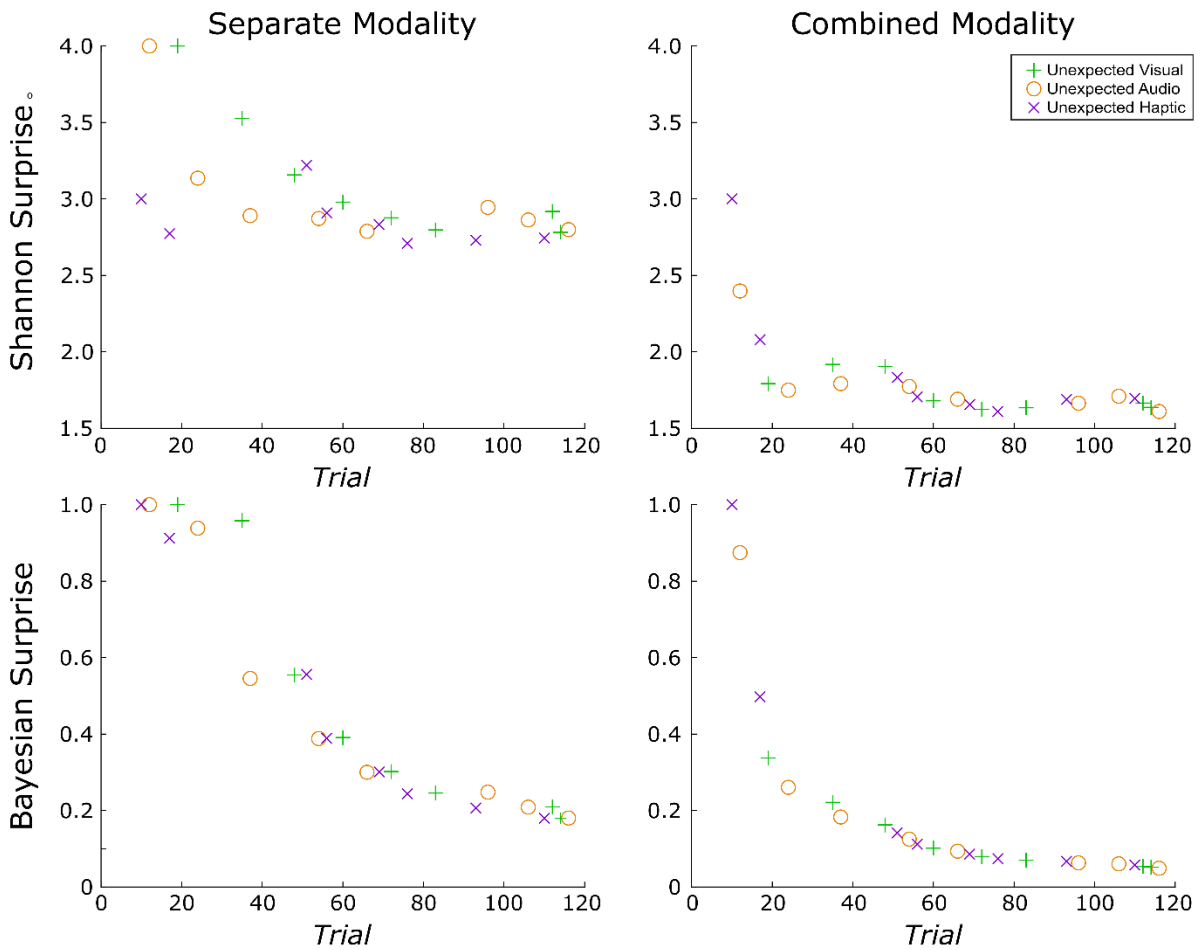

Fig. 2. Example of the surprise model specifications from a single subject in Dataset 1. *Surprise was quantified along two dimensions each with two levels. First, surprise was quantified according to each of two different formulas: (1) Shannon surprise, which is given by the inverse log of the probability of an unexpected event prior to its occurrence and (2) Bayesian surprise, which quantifies the difference in this probability and the updated probability after the unexpected event*

has occurred. Next, surprise was computed separately for each modality or combined (such that an unexpected haptic event is less surprising following an unexpected visual event). While the rate of decay is similar for combined modality models calculated using either surprise term, Shannon and Bayesian surprise differ somewhat when calculated separately for each modality. Namely, the decay is less rapid for Shannon surprise and is more affected by variations in the number of trials between successive unexpected events of the same variety.

Notably, both Shannon and Bayesian surprise contain the prior probability of an event and are therefore correlated (though they can be potentially disentangled through experimental instructions, as in O'Reilly et al., 2013). The main difference between the terms is that if a substantial number of standard trials occur before a given unexpected event, Shannon surprise can increase relative to the preceding unexpected event. By contrast, Bayesian surprise is always strictly monotonically decreasing.

Beyond the method for quantifying surprise (Shannon vs. Bayesian), in a dataset that contains unexpected events originating in different modalities, a second question is whether surprise is modeled commonly across modalities or for each modality separately (Wessel & Huber, 2019). This consideration has a substantial impact on the resulting surprise values. In the combined model, the surprise values decay even more rapidly as an unexpected event in the auditory modality is deemed less surprising even if it follows an unexpected event in the visual modality. Wessel and Huber (2019) modeled Bayesian surprise for both common and separate models and found that frontocentral P3 amplitude was better predicted by the separate model, suggesting that frontal cortex separately accounts for these various sources of surprise. (For a replication and extension of this work with Dataset 1, please refer to the Appendix.) Of main interest, the present work

provides a first examination of whether FC β-bursts relate to surprise. To this end, we again perform a model comparison that does not only compare Shannon vs. Bayesian surprise, but also compares separate vs. common surprise models across sensory modalities.

To complement the mean-based approach that examined RTs as function of Event Type and Block (detailed in the previous subsection), we also fit surprise values to RTs at the single-trial level. To do so, standardized (*z*-scored) surprise values were regressed onto standardized (*z*-scored) RTs using robust regression [in MATLAB, robustfit()] to generate beta weights for each participant. Group-level inference was drawn on the resulting beta weights using Bayesian one-sample Wilcoxon-signed rank tests to assess whether the surprise values reliably fit the data.

β-Burst extraction. Before identifying β-bursts, we minimized the potential for volume conduction by transforming the data to a reference-free montage via the current-source density (CSD) method (Perrin et al., 1989; Tenke & Kayser, 2005).

β-bursts were identified in the same manner as described by Shin et al. (2017) and Wessel (2020). The only exception is that we used a 2× median power threshold (in lieu of a 6× median power threshold) based on Enz et al.'s (2021) specification of optimal settings for β-burst detection. The description is adapted from Shin et al. (2017) as implemented Wessel (2020):

First, each electrode's data were convolved with a complex Morlet wavelet of the form:

$$w(t,f) = A \exp\left(\frac{t^2}{2\sigma_t^2}\right) \exp(2i\pi f t), \qquad (3)$$

with $\sigma = \frac{m}{2\pi f}$, $A = \frac{1}{\sigma}\sqrt{2\pi}$, and $m = 7$ (cycles) for each of 15 evenly spaced frequencies spanning the β-band (15–29 Hz). Time–frequency power estimates were extracted by calculating the squared

magnitude of the complex wavelet-convolved data. These power estimates were then epoched relative to the events in question (ranging from −500 to +2000 ms with respect to the cue in the CMO task, and -500 to +1000 ms with respect to signal onset in the SST). Individual β-bursts were defined as local maxima in the trial-by-trial β-band time–frequency power matrix for which the power exceeded a set cutoff of 2× the median power (Enz et al., 2021) of the entire time–frequency epoch power matrix for that electrode (i.e., the median thresholding was performed across all epochs). Local maxima within each epoch were identified using the MATLAB function imregional().

β-Burst analyses in the CMO tasks. To examine whether FC β-bursts were elevated following unexpected events and to potentially gain a better understanding of the time course of the β-bursts, we adopted a sliding window approach in place of the bin-based approaches used in prior work (e.g., Wessel, 2020). For this, we cycled through each sample beginning -100 ms prior to the onset of the cue and +500 ms after its onset and counted the number of bursts occurring within +/- 25 ms of the sample (with one sample corresponding to 2 ms of data). We then converted to burst rate by summing the number of bursts across trials and dividing by the number of trials. This process was completed for each of the FC electrodes of interest (FC1, FCz, FC2, C1, Cz, and C2). After this, we used the baseline period (-100 to 0 ms) to calculate the percent change in burst rate and to convert to percent change from baseline for each electrode. The resulting values were averaged across the FC electrodes. For these and all subsequent analyses, standard event trials that were immediately preceded by unexpected event trials were excluded. The data were then compared across each Event Type (standard, unexpected audio, unexpected visual, unexpected haptic). First, we used frequentist one-way repeated-measure ANOVAs over each time point

comparing percent change in burst rate across the various event types. Then, we used frequentist paired samples *t*-tests to compare each unexpected event type to the standard event. The initial, pre-defined alpha-level of .05 was used for these tests. The alpha-level was then adjusted for multiple comparisons via the FDR procedure (Benjamini et al., 2006) correcting for the number of tests (one for the ANOVA, three for the paired *t*-tests in Dataset 1, and two for the paired *t*-tests in Dataset 2) and the number of timepoints (250).

Next, the relationship between β-burst rate and surprise was explored. In each dataset, we looked at the association between the number of β-bursts and surprise values on (non-rejected) trials containing unexpected events in two different time ranges. After the results in Dataset 1 regarding the main research question concerning FC β-bursts were known, we explored these relationships within a specific time window containing the time period of elevated β-bursts. For this, we extracted the number of β-bursts between +75 and +200 ms following each unexpected event. Both the number of bursts within these search windows and the surprise values (again for each type of surprise and for separate and combined modality considerations) were standardized as *z*-scores and a beta weight was computed using robust regression (with the robustfit() function in MATLAB) for each subject. To draw inferences at the group-level, the resulting individual beta-weights were compared against zero using Bayesian one-sample Wilcoxon signed-rank tests. We here consider the results of Dataset 1 to be purely exploratory, whereas we consider any potentially replicated results in Dataset 2 to provide initial, confirmatory evidence.

We then examined the relationship between RTs and β-bursts in each dataset using the above single-trial level approaches used to relate surprise and β-bursts. For these analyses, we considered the specific time range (+75 to +200 ms following the event) and the full cue-to-target interval (0 to +500 ms) in both datasets.

β-Burst analysis in the SST. Lastly, we examined the dynamics of FC β-bursts in the SST (combined across Datasets 1 and 2) using the sliding window approach from the CMO task to compare β-bursts on successful stop trials to matched Go trials as well as to failed stop trials.

RESULTS

Behavior

The RT results of Dataset 1 closely matched those previously reported for Dataset 2 (Wessel & Huber, 2019) in all respects. The Bayesian RM-ANOVA on Event Type (standard, unexpected audio, unexpected visual, unexpected haptic) and Block (1, 2, 3, 4) indicated strong evidence for main effects of Event Type (BF_{10} = 7.02 x 10^5) and of Block (BF_{10} = 6.40 x 10^9). Strong evidence was also indicated for the Event Type X Block interaction over a model with only the two main effects (BF_{10} = 258.4). Most importantly, the basic comparisons between each type of unexpected event and standard events echoed the finding that all types of unexpected events induce RT slowing, but that — consistent with the notion of surprise adaptation — these differences wane over time. This was apparent as unexpected visual and unexpected auditory events both showed strong evidence of slowing compared to standard events in the first block (Unexpected audio: BF_{10} = 49.5; Unexpected visual: BF_{10} = 2.47 x 10^5). Likewise, we found that Unexpected haptic events also showed this slowing in the first block (BF_{10} = 4.51). In Block 2, a much-diminished RT slowing remained following the unexpected visual events (BF_{10} = 4.51); however, none of the other unexpected events in Block 2 and onwards showed evidence of RT slowing (BFs_{01} > 1). Thereby, the behavioral RT results replicated Wessel and Huber (2019) and extended them to the haptic domain.

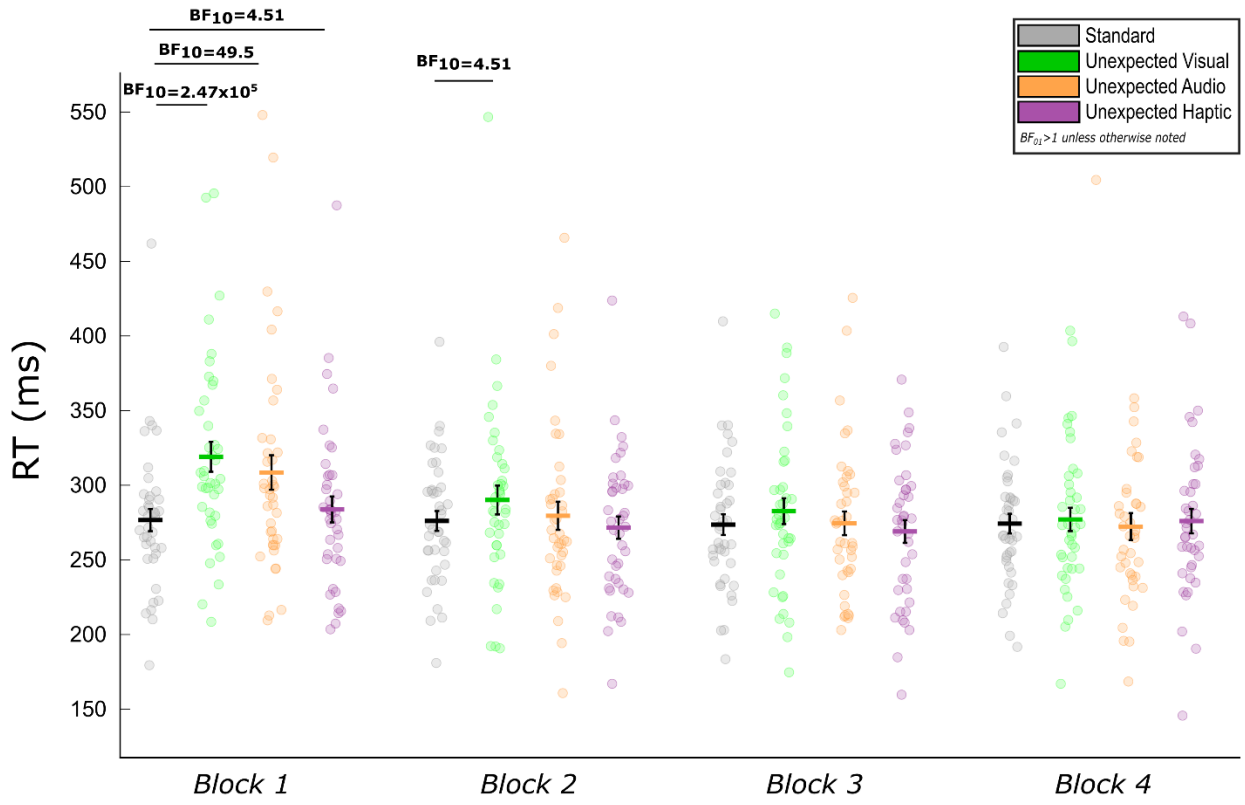

Fig. 3. Mean RTs as a function of Event Type and Block for the trimodal cross-modal oddball task of Dataset 1. *Paired Bayesian t-tests indicated RT slowing following all three types of unexpected events in the first block. Consistent with the notion of surprise, these differences quickly dissipated as suggested by the lack of differences in subsequent blocks (and the attenuated difference following unexpected visual events in the second block). Black error bars indicate SEM.*

The single-trial fits of RT and surprise lent themselves to similar conclusions as the mean-based approach to RTs, with some additional insights. There was strong evidence to suggest that Shannon surprise with separate modality terms positively predicted RTs (BF_{10} = 39.74), whereas there was moderate evidence against Shannon surprise with common modality terms predicting the data (BF_{01} = 4.57). Similarly, there was strong evidence that Bayesian surprise with separate modality terms positively predicted RTs (BF_{10} = 22.14), but only anecdotal evidence to suggest

this for Bayesian surprise with common modality terms (BF_{10} = 2.11). Thus, participants' RTs appeared to follow both types of surprise, provided their values represented surprise separately for each type of unexpected event.

For mean error rates, there was a main effect of Event Type on error rate (moderate evidence, BF_{10} = 6.68) but not of Block (strong evidence, BF_{01} = 20.83), nor was there an Event Type x Block interaction (strong evidence, BF_{01} = 2172). The mean percent error rates for each Event Type were as follows: Standard: 1.86%, Unexpected auditory: 0.17%, Unexpected visual: 1.09%, and Unexpected haptic: 1.41%. Follow-up *t*-tests on Event Type indicated that the main effect was driven by the lower number of errors following unexpected auditory events compared to standard events (BF_{10} = 3.19 x 10^5). The evidence did not suggest that the other types of unexpected events differed from the standard (unexpected visual: BF_{01} = 2.01, unexpected haptic: BF_{01} = 7.52), nor did they differ from the unexpected auditory event (unexpected visual: BF_{01} = 1.22, unexpected haptic: BF_{01} = 9.91). This outcome contrasts those for Dataset 2 which showed increased error rates following unexpected auditory and visual events that remained stable across blocks. However, error and miss trials were generally rare and not considered in the EEG analyses.

For mean miss rates, the results were in line with the null findings of Dataset 2. Strong evidence was found for a lack of differences regarding Event Type (BF_{01} = 126.0), Block (BF_{01} = 10.28), and the Event Type x Block interaction (BF_{01} = 315.9).

The SST also closely followed those from Dataset 2. Mean Go RT = 535 ms, mean failed stop RT = 464 ms, mean SSRTi = 252 ms, and mean *p*(inhibit) = .52 (compared to Dataset 2: mean Go RT = 520 ms, mean failed stop RT = 444 ms, mean SSRTi = 252.00, and *p*(inhibit) = .51).

EEG

FC β-bursts are increased following unexpected events in all three modalities. In Dataset 1, significantly increased β-bursting followed each type of unexpected event (FDR-corrected to p <.05). First, significant differences across all event types were detected with one-way RM-ANOVAs from 82-136 ms after event onset. More importantly, comparing the sliding window trace for each unexpected event to the standard revealed elevated β-bursts following unexpected auditory event from 96-152 ms, following unexpected visual event from 88-170 ms, and following unexpected haptic events from 44-140 ms.

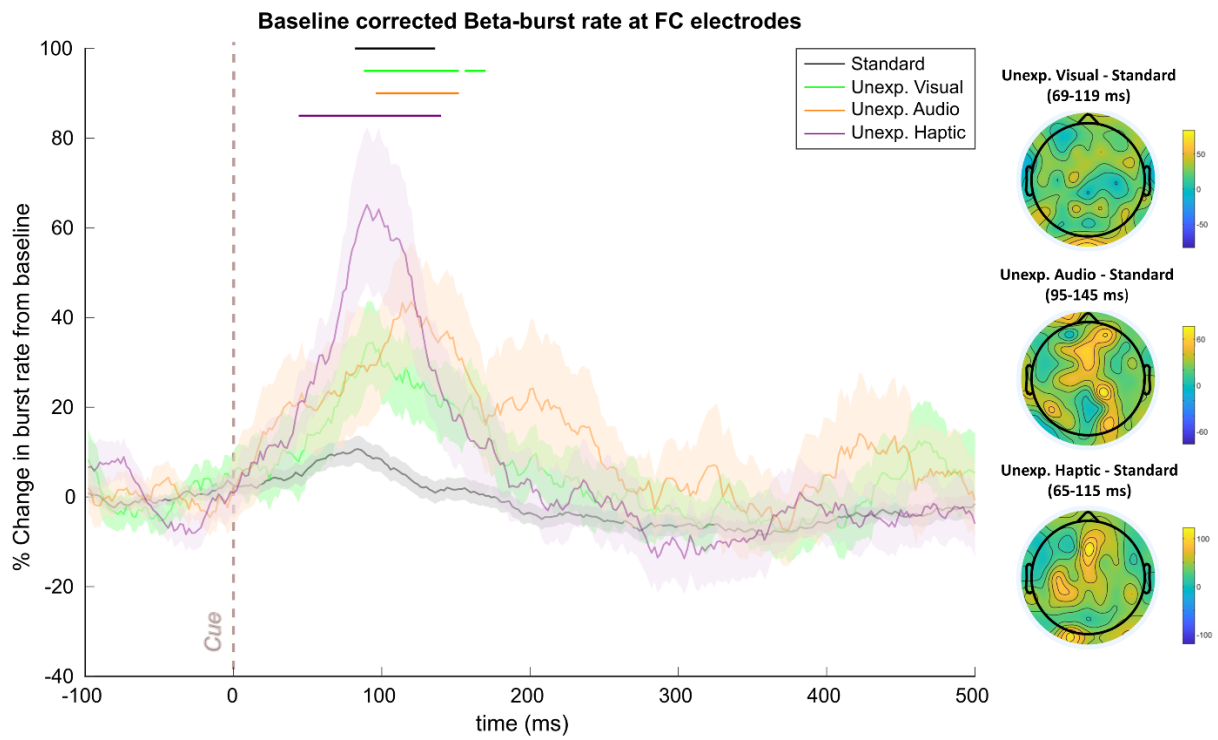

Fig. 4. FC β-bursts following unexpected events in Dataset 1 (n = 40). *(Left) Depicts the percent change in β-burst rate relative to baseline for +/- 25 ms sliding windows calculated for each 2 ms timepoint. An increase in β-bursts at FC sites was evident following unexpected events in all three modalities at early latencies. Sliding window timepoints with significant differences (FDR-*

corrected, p = .05) across event types are denoted by horizontal lines at the top of the plot (black: rm-ANOVAs across all event types, green: unexpected visual vs. standard, orange: unexpected auditory vs. standard; purple: unexpected haptic vs. standard). Shaded regions indicate SEM. (Right) Scalp topography differences depicting the % change in β-bursts at all electrodes in the +/- 25 ms window surrounding the maxima for each unexpected event type identified with the sliding window technique relative to the same time period for the standard event.

In Dataset 2, the RM-ANOVA detected significant differences across conditions from 110-232 ms. These sliding windows coincided virtually identically with those identified for the unexpected auditory events compared to the standard event (108-232 ms). Although unlike in Dataset 1, we did not find significant increases following unexpected visual events by themselves, this was a consequence of the FDR correction. Without it, (i.e., using alpha=.05 with two-sided tests), β-bursts were again increased following unexpected visual events (18-46ms). This deviation from Dataset 1 notwithstanding, the overall results strongly suggest that, as predicted, β-bursts are generally increased following unexpected events.

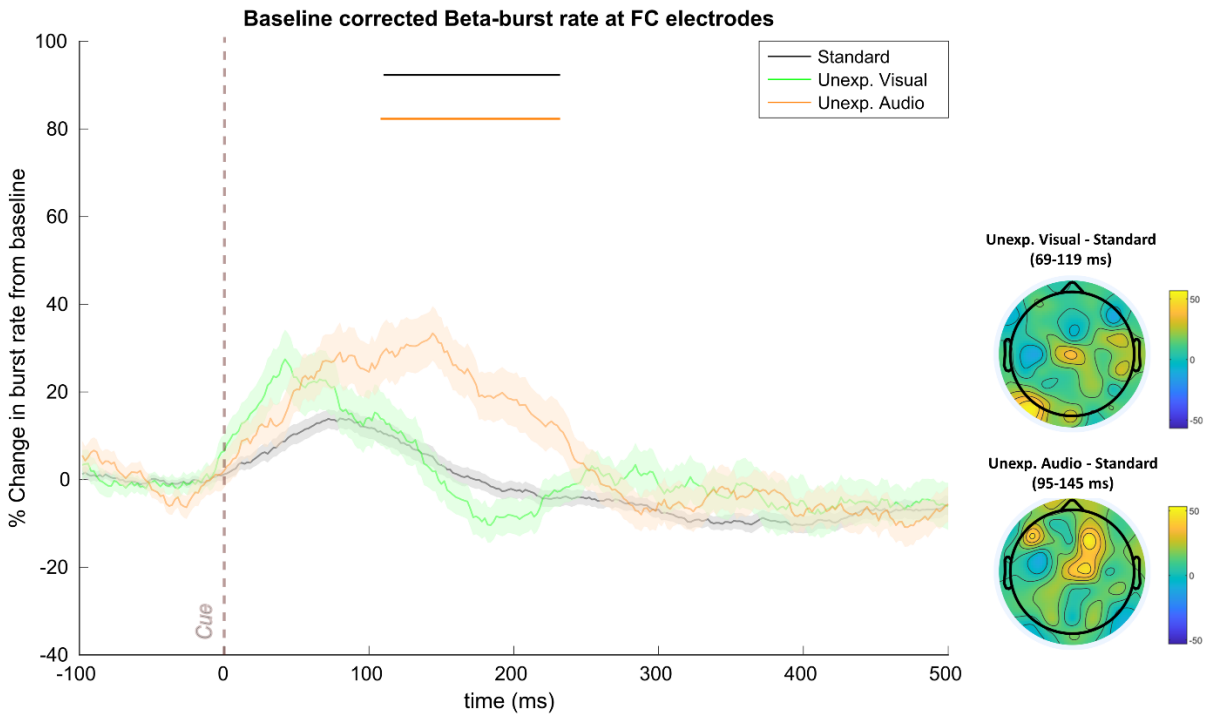

Fig. 5. FC β-bursts following unexpected events in Dataset 2 (n=55). *(Left) Depicts the percent change in β-burst rate relative to baseline for +/- 25 ms sliding windows calculated for each 2 ms timepoint. An increase in β-bursts at FC sites was evident following unexpected auditory events. The numerical increase in β-burst rate following unexpected visual events did not achieve significance. Sliding window timepoints with significant differences (FDR-corrected, p = .05) across event types are denoted by horizontal lines at the top of the plot (black: rm-ANOVAs across all event types, green: unexpected visual vs. standard, orange: unexpected auditory vs. standard). Shaded regions indicate SEM. (Right) Scalp topography differences depicting the % change in β-bursts at all electrodes in the +/- 25 ms window surrounding the maxima for each unexpected event type identified with the sliding window technique relative to the same time period for the standard.*

Early FC β-bursts reflect modality-specific Shannon surprise terms. We used Dataset 1 for exploratory analyses of potential relationships between FC β-bursts and surprise. We then aimed to replicate any such findings using Dataset 2. After having identified that FC β-bursts were increased following unexpected events in Dataset 1, we considered these relationships within a specific time range that contained the period during which unexpected events were followed by significant increases in β-bursts (75 to 200 ms after event onset). The individual-subject beta-weights from these analyses are plotted in Fig. 6*a*. Shannon surprise with separate modality terms for each modality was positively associated with β-bursting as *BF* indicated moderate evidence that the mean beta weight at the group-level was above zero (BF_{10} = 4.15). Contrastingly, *BFs* for the other surprise models indicated moderate evidence for no relationship (Bayesian surprise/separate terms: BF_{01} = 5.38, Bayesian surprise, combined terms: BF_{01} = 4.05, Shannon surprise/combined terms: BF_{01} = 5.62).

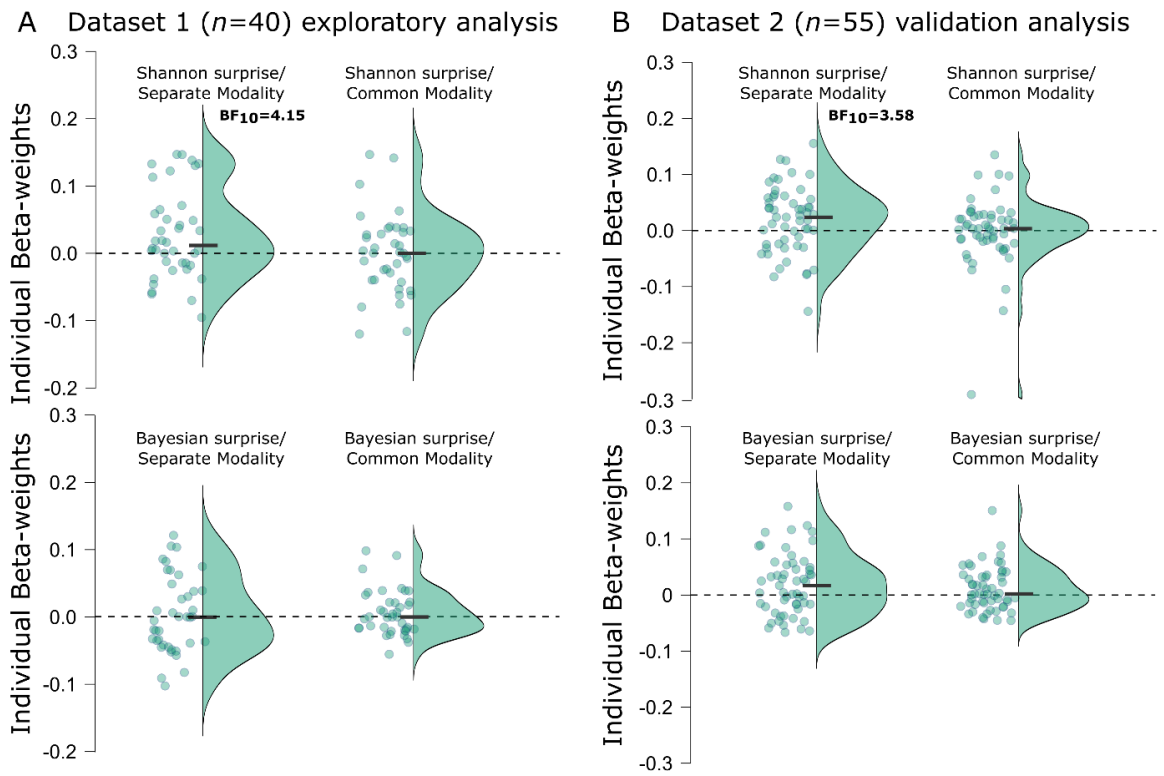

Fig. 6. Individual beta-weights from the various z-scored surprise single-trial model values fitted to z-scored β-bursts from 75 - 200 ms following unexpected events. a *Points represent mean beta-weights from individual subjects estimated via robust regression for each surprise model in Dataset 1. Half violin plots depict the distribution of beta-weights. Black bars indicate mean beta-weights.* ***b*** *The same as in a but for Dataset 2 which was used to validate potential findings in Dataset 1. Reported* BF_{10}*s correspond to moderate evidence in favor of the alternative hypothesis.* BF_{10}*s* < 3 *are not shown here (but are reported in the main text).*

To confirm these exploratory findings, we completed the same analyses using Dataset 2. The individual-subject beta-weights are plotted in Fig. 6*b*. Just as in Dataset 1, there was moderate evidence that Shannon surprise with separate model terms positively predicted FC β-bursting (BF_{10} = 3.58). While there was again moderate evidence for no relationship regarding Shannon surprise with combined modality terms (BF_{01} = 6.54), this time, there was anecdotal evidence suggesting positive relationships for Bayesian surprise with separate terms (BF_{10} = 2.53) and Bayesian surprise with combined terms (BF_{10} = 1.29). Here, it may be worth mentioning that in the trimodal dataset, any given unexpected event was less frequent than in the bimodal dataset. Consequently, the difference between Shannon surprise and Bayesian surprise values should be relatively more pronounced in Dataset 1 owing to the longer stretches of trials between successive unexpected events of the same ilk. This could potentially explain why Bayesian surprise models appeared to show some hint of a relationship in Dataset 2 that was not observed in Dataset 1. Either way, Shannon surprise with modality-specific terms consistently outperforms the other models across both datasets.

No observed relationships between FC β-bursts and RT in the CMO task. We next investigated relationships between RT and FC β-bursts. No reliable associations were found between the number of FC β-bursts and RTs on unexpected event trials in either dataset with either time range (Dataset 1, full time range: BF_{01} = 5.56, constrained time range: BF_{01} = 4.93; Dataset 2, full time range: BF_{01} = 5.41, constrained time range: BF_{01} = 6.67). Neither were reliable associations found on standard event trials (Dataset 1, full time range: BF_{10} = 2.60, constrained time range: BF_{01} = 5.32; Dataset 2, full time range: BF_{01} = 6.76, constrained time range: BF_{01} = 4.02).

Stop-signal related FC β-bursts are increased later than those after unexpected events. As can be seen in Fig. 7, FC β-bursts were also increased following the stop signal. In the SST (from Datasets 1 and 2, n = 94), FC β-bursts were increased on successful stop trials compared to matched Go trials from 174-272 ms. This replicates prior work documenting increased β-bursting at frontal sites following the stop signal (Wessel, 2020; Jana et al., 2020). Interestingly, no time point differences were found for successful compared to failed stop trials. However, the peak burst rate latency for successful stops clearly preceded that for failed stops (Fig. 7). This parallels the main finding involving FC P3 in which the amplitude peaks earlier on successful stop trials (e.g., Kok et al., 2004) and would suggest that the process related to FC β-bursts begins (or at least comes to fruition) sooner on these trials. It is perhaps also interesting that the implicated time range occurred later than the time ranges in which we found increased FC β-bursting following unexpected events in the CMO task, which spanned from 44-232 ms across the various event types. Still, in each task, FC β-burst differences emerged earlier than the earliest differences in the corresponding FC P3, which for the sake of comparison, are placed here in Fig. 8 (for

methodological details, see Appendix). This suggests that these signatures may represent separate processes.

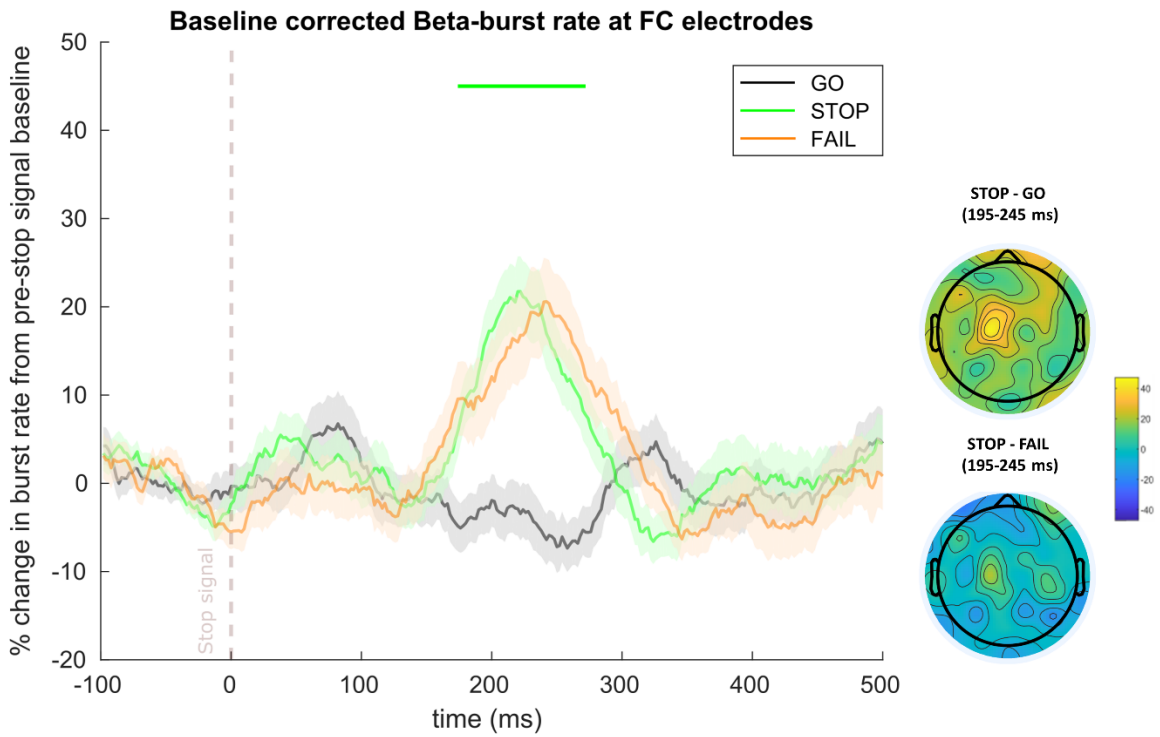

Fig. 7. FC β-bursts following the stop signal in the SST (n=94, combined from Datasets 1 and 2). *Depicts the percent change in β-burst rate relative to baseline for +/- 25 ms sliding windows calculated for each 2 ms timepoint. β-bursts at FC sites were increased on successful stop trials (stop) compared to matched Go (go). Failed-stop trials (fail) did not differ from successful stop trials. Sliding window timepoints with significant differences (after FDR correction) across trial types are denoted by horizontal lines at the top of the plot (green: successful stop vs. matched go). Shaded regions indicate SEM. (Lower Right) Scalp topography differences depicting the % change in β-bursts at all electrodes in the +/- 25 ms window surrounding the maximum for successful stop compared to matched timepoints on go and failed-stop trials.*

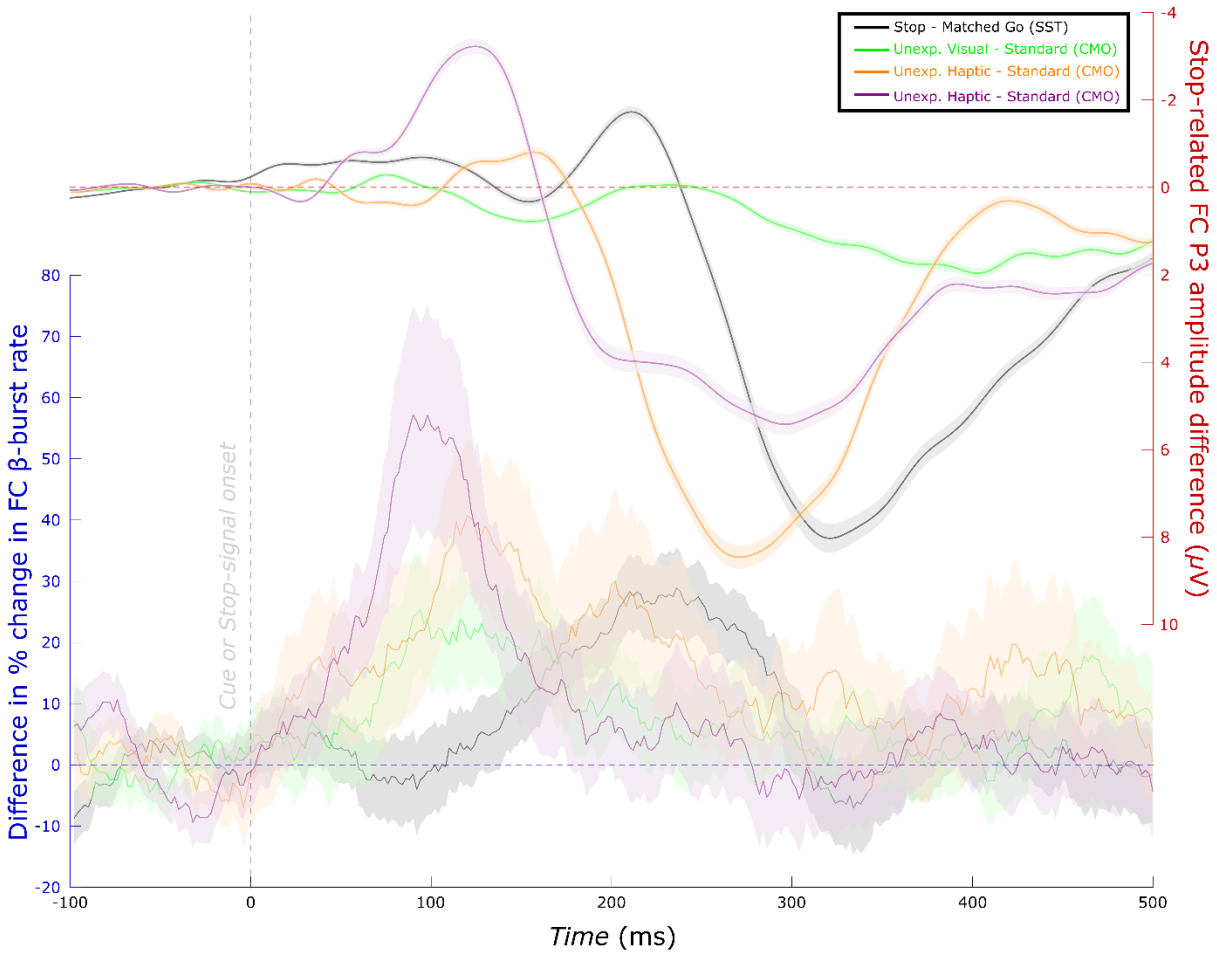

Fig. 8. Time-course of differences in FC β-burst rate compared to FC P3 (Dataset 1, n=39). *(Left Scale) Differences in the percent change in β-burst rate for successful stop trials compared to matched go (from Fig. 7, but only involving Dataset 1 participants) as well as unexpected events relative to standard (from Fig. 4). (Right Scale) The same differences for FC P3. For this, the SST was used as a functional localizer to isolate an IC corresponding to the FC stop-signal P3 in the merged dataset (i.e., the CMO and SST in Dataset 1). Visual inspection indicates that FC β-burst differences precede the corresponding FC P3 differences. Unexpected event differences generally also precede stop differences (excepting the FC P3 for unexpected visual events).*

DISCUSSION

We found clear and consistent support for our prediction that FC β-bursts would be increased following unexpected events. In Dataset 1, which included unexpected events in auditory, visual, and haptic modalities, increased β-bursting at frontal electrode sites was evident in all three modalities. In Dataset 2 (from Wessel & Huber, 2019), which included unexpected events in the auditory and visual modalities, increased FC β-bursting was evident following unexpected auditory events, and, numerically, following unexpected visual events as well. To our knowledge, this represents the first investigation of β-bursts following unexpected events.

Jones and colleagues have recently suggested a role for β-bursts in the detection of sensory events. In particular, Shin et al. (2017) showed that β-bursts over somatosensory cortices originating 300 to 100 ms before tactile stimulus delivery impaired perception whereas Law et al. (2022) showed that β-bursts contemporaneous with stimulus delivery aided perception. While we did not explicitly explore the consequences of β-bursts on perception, our results suggest that FC β-bursts may also play a role in stimulus detection and perhaps in registering their salience. The finding of early increased FC β-bursting following unexpected events compared to standard events already suggests that these bursts may play a role in the detection of infrequent events. However, our finding that these bursts also scale with Shannon surprise on just the subset of trials with unexpected events joins and expands upon this finding to suggest that this infrequency-representation happens at very fine-grained scale (capturing trial-to-trial deviations in expected probabilities).

Across both datasets, FC β-bursting was linked to a specific type of surprise: Shannon surprise with separate terms for each modality. Although largely correlated, Shannon surprise and Bayesian surprise differ mainly in that an unexpected event can have a higher surprise value than

its predecessor with a sufficiently long stretch of intermediate expected events. Our experimental design did not explicitly attempt to dissociate the two types of surprise, although when assuming that unexpected events in different modalities are separately surprising, the types of surprise should be less correlated in Dataset 1 which had three types of unexpected events compared to Dataset 2 which had two (given the same overall probability of any type of unexpected event). Given that Bayesian surprise and Shannon surprise were largely correlated in the datasets, however, it is even more interesting that FC β-bursts specifically correlated with Shannon surprise in both cases, and to a consistently lesser extent with Bayesian surprise. It is unlikely that this dissociation is explainable in terms of differing degrees of sensitivity to detect either relationship as both types of surprise were predictive of RT and the whole-brain EEG data corresponding to the FC P3 response at the single-trial level. Prior work has indicated that Shannon surprise and Bayesian surprise relate to at least somewhat distinct neural processes. For instance, using fMRI, O'Reilly et al. (2013) identified activity within posterior parietal cortex as representing Shannon (i.e., updating, as they refer to it) whereas activity in anterior cingulate cortex and pre-supplementary motor area uniquely represented Bayesian surprise. Scalp-surface EEG studies suggest that whereas FC P3 better characterizes Bayesian surprise, Shannon surprise is better characterized by centro-parietal P3 (Mars et al., 2008; Kolossa et al., 2015; Seer et al., 2016; Wessel & Huber, 2019). Interestingly, the present results suggest that FC β-bursts might represent a unique frontal cortex neural correlate of Shannon surprise and one that emerges sooner than the P3 components. To our knowledge, this represents the first demonstration of a signature of Shannon surprise over frontal cortex. Presumably, this early detection of infrequent events or surprise could serve to pave the way for rapid adjustments to behavior and cognition (O'Reilly et al., 2013; Wessel & Aron, 2017; Diesburg & Wessel, 2021).

The time course of this increase in FC β-bursts and its relation to surprise was further interesting. Although the sliding window approach we employed to analyze β-bursts still introduces temporal uncertainty as to the precise timing with which increased β-bursting begins, we could at least be confident that FC β-bursts were elevated soon after the presentation of the unexpected event and well before 200 ms. This is important in establishing FC β-bursts as a potentially early signature because, notably, the putative onset of the FC P3 process within the context of action stopping occurs much later, around 200 ms (Wessel & Aron, 2015). We further show that increased FC β-bursting began well before the FC stop-signal P3 and before the FC P3s in the same CMO task. These findings offer important insight and constraints with respect to the potential processes this early FC β-burst signature might relate to within a couple of our theoretical frameworks. Wessel and Aron's (2017) adaptive re-orienting theory of attention and Diesburg and Wessel's human pause-then-cancel model (2021) commonly propose multi-stage models whereby an early stage is characterized by global inhibition of the motor system brought about by the detection of unexpected or otherwise salient, behaviorally relevant events which is then followed by a later stage in which more strategic adjustments and updates to ongoing motor and cognitive programs occur. Based on the timing of various functional neurophysiological signatures and their relation to behavior, Diesburg and Wessel (2021) have proposed certain functional signatures to be associated with either this early or late inhibitory stage. For instance, studies involving single-pulse TMS stimulation of M1 regions responsible for muscles irrelevant to the task at hand both within action stopping contexts (i.e., the SST or its variants) and within following unexpected events have estimated global inhibition to begin around 150 ms, thus providing the main functional signature of the pause phase. Other signatures such as brief decreases in EMG around this time (Jana et al., 2020; Raud & Huster, 2017; Raud et al., 2020; Tatz et al., 2021) or the still earlier,

transitory decreases in isometric force contractions (Novembre et al., 2018) also likely relate to this stage. By contrast, the main purported neurophysiological correlate of the cancel phase is the FC P3 signature which has been tied to successful response inhibition in the SST and RT slowing following unexpected events. However, a direct neural correlate of the pause phase with precise timing such as EEG or magnetoencephalography is lacking. Moreover, based on previously observed timings of increased FC β-bursting following the stop signal (Jana et al., 2020; Wessel, 2020), it remained unclear which processing stage this inhibitory signature better related to, or whether it better indexed proactive inhibitory control. In the primarily reactive context of the CMO task, elevated FC β-bursts emerged soon after event onset and were clearly consistent with the timing of the pause phase but not the cancel phase. In the SST involving the same individuals, elevated β-bursting emerged somewhat later (~178 ms) but still prior to 200 ms and the emergence of the stop-signal P3. This timing is rather intermediate to the ~120 ms timing found by Jana et al. (2020) and the ~200 ms timing found by Wessel (2020), but nevertheless shifts the evidence in favor of a timing more consistent with the pause phase.

Given that FC β-bursting and the subsequent FC P3 following unexpected events considerably outpaced the same signatures in the SST (except, possibly the P3 for visual unexpected events), an intriguing possibility is whether surprise accelerates the inhibitory process. Some initial evidence for this comes from Iacullo et al. (2020) who examined cortical-spinal excitability while participants responded to imperative stimuli that were quickly followed by standard tones, infrequent/expected tones, or novel/unexpected sounds. Critically, they found global motor suppression to occur earlier following novel/unexpected sounds compared to infrequent/expected tones. In contrast to surprising events, the SST contains not just the reactive inhibitory control brought about by the infrequent stop-signal itself, but also proactive inhibitory

control, or strategic adjustments in anticipation of the stop-signal (Elchlepp et al., 2016; Wessel, 2018b). To better capture proactive control, researchers have created variants of the SST that include certain go trials (in contrast to the default, maybe stop trials). However, fMRI studies that have done so have implicated BOLD responses in the same regions (Chikazoe et al., 2009; Jahfari et al., 2010), and EEG studies have likewise implicated some of the same event-related potentials, including FC P3, in both types of control (Elchlepp et al., 2016; Raud & Huster, 2017). Soh et al. (2021) found increased sensorimotor β-bursts on maybe stop compared to certain go trials, a difference that was present even before trial onset. Interestingly, Muralidharan et al.'s (2022) recent work modeling frontal β-bursts in the SST suggested that these bursts increased the decisional threshold necessary for the Go response. Taken together, studies on the SST suggest that some of the same processes subserve proactive and reactive inhibitory control. If so, it would seem plausible that these processes might take place more rapidly when proactive control is minimal, as in the case of surprising events. From the standpoint of rapidly allocating resources and adjusting behavior, this would indeed be an adaptive feature as, at least in most real-world settings, the optimal course of action (or inaction) cannot be known in advance of the surprising event but instead must be urgently gleaned after their occurrence. Most basically, we herein demonstrate that frontal β-bursts occur in reactive contexts.

In the present task designs, FC β-bursts were not directly related to the observed motor slowing. One possibility is that β-bursts reflect an early processing stage that only indirectly relates to RT. Within the proposed pause phase (Diesburg & Wessel, 2021), information must pass through cortex and multiple subcortical structures before arriving at primary motor cortex. By contrast, the proposed cancel phase is argued to more directly relate to actual behavioral adjustments. Subsequently, the correspondence of FC β-bursts with RT may have been too subtle

to detect a relationship (even as RT is a highly variable measure itself), even though this lack of relationship could still be consistent with pause phase roles of salient event detection or otherwise triggering inhibition. In addition, the FC P3, which is a prominent signature of the cancel phase, exhibited strong correspondences with RT following each type of unexpected event (see *Fig.* A2). Another reason for not finding a connection between FC β-bursts and RT could owe to the nature and timing of our CMO task. In our task, unexpected events occurred as a part of a cue that occurred 500 ms before the imperative stimulus. Thus, any early inhibition prompted by the unexpected events might have been overcame by the time the stimulus appeared. Rather, the timing of our task may have been more optimal for capturing the impact of the cancel phase on inhibition, and indeed we found relationships between RT and FC P3. In hindsight, the timing of increased FC β-bursting and subsequent sensorimotor β-bursting might have also occurred too soon. For instance, Little et al. (2019) showed that movement was only disrupted by sensorimotor β-bursts that occurred just before the response. Here, responses occurred even sometime after target onset (as participants complete a choice RT task). Given that these issues could have compounded in the present task design, it is interesting to consider whether a relationship between β-bursts and behavior might be established in a task in which unexpected events occur during movement which could be assessed for instance by presenting unexpected events just after the first increase in electromyographic activity. Regardless, if global inhibition serves to promote rapid action adjustments in the first place, it would seem plausible that this process might be more active when actions are already underway.

In sum, we have shown that unexpected events in three modalities (auditory, haptic, and visual) prompt increases in FC β-burst rate soon after their onset and before 200 ms. These β-bursts further appear to track the surprise (or trial to trial fluctuations in stimulus infrequency) of

these events separately for each modality and as indexed by Shannon surprise. We also show that FC β-bursts are accompanied by increases in sensorimotor β-bursts, especially at short latencies following their occurrence. Although we were unable to establish a relationship between FC β-bursts and RT, the overall results suggest that FC β-bursts may play an early role in inhibitory processes such as salient event detection and/or the triggering of the global inhibition characteristic of the pause phase.

Data Availability Statement

All data and analysis scripts will be deposited publicly on the OSF upon acceptance of the manuscript.

Acknowledgements

We thank Saara Engineer, Nathan Chalkley, Nathan Chen, and Kylie Dolan for their help with data collection.

Author contributions

Joshua R. Tatz: Conceptualization; Formal analysis; Investigation; Visualization; Writing – Original Draft, Writing – Review & editing. Alec Mather: Conceptualization; Investigation; Formal analysis. Jan R. Wessel: Conceptualization; Formal analysis; Funding acquisition; Investigation; Project administration; Supervision; Writing – Review & editing.

Funding Information

National Institutes of Health R01 NS102201 to JRW. National Institutes of Health R01 NS117753 to JRW.

Competing Interests

The authors declare no competing interests.

REFERENCES

Anidi, C., O'Day, J. J., Anderson, R. W., Afzal, M. F., Syrkin-Nikolau, J., Velisar, A., & Bronte-Stewart, H. M. (2018). Neuromodulation targets pathological not physiological beta bursts during gait in Parkinson's disease. *Neurobiology of disease*, *120*, 107-117.

Aron, A. R. (2011). From reactive to proactive and selective control: developing a richer model for stopping inappropriate responses. *Biol Psychiatry*, *69*(12), e55-68. https://doi.org/10.1016/j.biopsych.2010.07.024

Asplund, C. L., Todd, J. J., Snyder, A. P., Gilbert, C. M., & Marois, R. (2010). Surprise-induced blindness: a stimulus-driven attentional limit to conscious perception. *J Exp Psychol Hum Percept Perform*, *36*(6), 1372-1381. https://doi.org/10.1037/a0020551

Badry, R., Mima, T., Aso, T., Nakatsuka, M., Abe, M., Fathi, D., Foly, N., Nagiub, H., Nagamine, T., & Fukuyama, H. (2009). Suppression of human cortico-motoneuronal excitability during the Stop-signal task. *Clin Neurophysiol*, *120*(9), 1717-1723. https://doi.org/10.1016/j.clinph.2009.06.027

Baldi, P., & Itti, L. (2010). Of bits and wows: A Bayesian theory of surprise with applications to attention. *Neural Netw*, *23*(5), 649-666. https://doi.org/10.1016/j.neunet.2009.12.007

Bell, A. J., & Sejnowski, T. J. (1995). An information-maximization approach to blind separation and blind deconvolution. *Neural computation*, *7*(6), 1129-1159.

Benjamini, Y., Krieger, A. M., & Yekutieli, D. (2006). Adaptive linear step-up procedures that control the false discovery rate. *Biometrika*, *93*(3), 491-507. https://doi.org/10.1093/biomet/93.3.491

Boehler, C. N., Schevernels, H., Hopf, J.-M., Stoppel, C. M., & Krebs, R. M. (2014). Reward prospect rapidly speeds up response inhibition via reactive control. *Cognitive, Affective, & Behavioral Neuroscience*, *14*(2), 593-609.

Brainard, D. H. (1997). The Psychophysics Toolbox. *Spat Vis*, *10*(4), 433-436. https://www.ncbi.nlm.nih.gov/pubmed/9176952

Cai, W., Oldenkamp, C. L., & Aron, A. R. (2012). Stopping speech suppresses the task-irrelevant hand. *Brain Lang*, *120*(3), 412-415. https://doi.org/10.1016/j.bandl.2011.11.006

Chikazoe, J., Jimura, K., Hirose, S., Yamashita, K., Miyashita, Y., & Konishi, S. (2009). Preparation to inhibit a response complements response inhibition during performance of a stop-signal task. *J Neurosci*, *29*(50), 15870-15877. https://doi.org/10.1523/JNEUROSCI.3645-09.2009

Corbetta, M., & Shulman, G. L. (2002). Control of goal-directed and stimulus-driven attention in the brain. *Nat Rev Neurosci*, *3*(3), 201-215. https://doi.org/10.1038/nrn755

Delorme, A., & Makeig, S. (2004). EEGLAB: an open source toolbox for analysis of single-trial EEG dynamics including independent component analysis. *J Neurosci Methods*, *134*(1), 9-21. https://doi.org/10.1016/j.jneumeth.2003.10.009

Delorme, A., Palmer, J., Onton, J., Oostenveld, R., & Makeig, S. (2012). Independent EEG sources are dipolar. *PLoS One*, *7*(2), e30135. https://doi.org/10.1371/journal.pone.0030135

Delorme, A., Sejnowski, T., & Makeig, S. (2007). Enhanced detection of artifacts in EEG data using higher-order statistics and independent component analysis. *Neuroimage*, *34*(4), 1443-1449. https://doi.org/10.1016/j.neuroimage.2006.11.004

Diesburg, D. A., Greenlee, J. D., & Wessel, J. R. (2021). Cortico-subcortical beta burst dynamics underlying movement cancellation in humans. *Elife*, *10*. https://doi.org/10.7554/eLife.70270

Diesburg, D. A., & Wessel, J. R. (2021). The Pause-then-Cancel model of human action-stopping: Theoretical considerations and empirical evidence. *Neurosci Biobehav Rev*, *129*, 17-34. https://doi.org/10.1016/j.neubiorev.2021.07.019

Dutra, I. C., Waller, D. A., & Wessel, J. R. (2018). Perceptual Surprise Improves Action Stopping by Nonselectively Suppressing Motor Activity via a Neural Mechanism for Motor Inhibition. *J Neurosci*, *38*(6), 1482-1492. https://doi.org/10.1523/JNEUROSCI.3091-17.2017

Egner, T., Monti, J. M., & Summerfield, C. (2010). Expectation and surprise determine neural population responses in the ventral visual stream. *J Neurosci*, *30*(49), 16601-16608. https://doi.org/10.1523/JNEUROSCI.2770-10.2010

Elchlepp, H., Lavric, A., Chambers, C. D., & Verbruggen, F. (2016). Proactive inhibitory control: A general biasing account. *Cognitive Psychology*, *86*, 27-61.

Enz, N., Ruddy, K. L., Rueda-Delgado, L. M., & Whelan, R. (2021). Volume of beta-Bursts, But Not Their Rate, Predicts Successful Response Inhibition. *J Neurosci*, *41*(23), 5069-5079. https://doi.org/10.1523/JNEUROSCI.2231-20.2021

Feingold, J., Gibson, D. J., DePasquale, B., & Graybiel, A. M. (2015). Bursts of beta oscillation differentiate postperformance activity in the striatum and motor cortex of monkeys performing movement tasks. *Proc Natl Acad Sci U S A*, *112*(44), 13687-13692. https://doi.org/10.1073/pnas.1517629112

Fischer, A. G., & Ullsperger, M. (2013). Real and fictive outcomes are processed differently but converge on a common adaptive mechanism. *Neuron*, *79*(6), 1243-1255. https://doi.org/10.1016/j.neuron.2013.07.006

Friston, K. (2010). The free-energy principle: a unified brain theory? *Nat Rev Neurosci*, *11*(2), 127-138. https://doi.org/10.1038/nrn2787

Hakim, N., Feldmann-Wustefeld, T., Awh, E., & Vogel, E. K. (2021). Controlling the Flow of Distracting Information in Working Memory. *Cereb Cortex*, *31*(7), 3323-3337. https://doi.org/10.1093/cercor/bhab013

Horstmann, G. (2015). The surprise-attention link: a review. *Ann N Y Acad Sci*, *1339*, 106-115. https://doi.org/10.1111/nyas.12679

Iacullo, C., Diesburg, D. A., & Wessel, J. R. (2020). Non-selective inhibition of the motor system following unexpected and expected infrequent events. *Exp Brain Res*, *238*(12), 2701-2710. https://doi.org/10.1007/s00221-020-05919-3

Jahfari, S., Stinear, C. M., Claffey, M., Verbruggen, F., & Aron, A. R. (2010). Responding with restraint: what are the neurocognitive mechanisms? *J Cogn Neurosci*, *22*(7), 1479-1492. https://doi.org/10.1162/jocn.2009.21307

Jana, S., Hannah, R., Muralidharan, V., & Aron, A. R. (2020). Temporal cascade of frontal, motor and muscle processes underlying human action-stopping. *Elife*, *9*. https://doi.org/10.7554/eLife.50371

Kim, H. (2014). Involvement of the dorsal and ventral attention networks in oddball stimulus processing: A meta-analysis. *Human brain mapping*, *35*(5), 2265-2284.

Kok, A., Ramautar, J. R., De Ruiter, M. B., Band, G. P., & Ridderinkhof, K. R. (2004). ERP components associated with successful and unsuccessful stopping in a stop-signal task. *Psychophysiology*, *41*(1), 9-20. https://doi.org/10.1046/j.1469-8986.2003.00127.x

Kolossa, A., Kopp, B., & Fingscheidt, T. (2015). A computational analysis of the neural bases of Bayesian inference. *Neuroimage*, *106*, 222-237.

Law, R. G., Pugliese, S., Shin, H., Sliva, D. D., Lee, S., Neymotin, S., Moore, C., & Jones, S. R. (2022). Thalamocortical mechanisms regulating the relationship between transient beta events and human tactile perception. *Cerebral Cortex*, *32*(4), 668-688.

Lee, T. W., Girolami, M., & Sejnowski, T. J. (1999). Independent component analysis using an extended infomax algorithm for mixed subgaussian and supergaussian sources. *Neural Comput*, *11*(2), 417-441. https://doi.org/10.1162/089976699300016719

Levy, B. J., & Wagner, A. D. (2011). Cognitive control and right ventrolateral prefrontal cortex: reflexive reorienting, motor inhibition, and action updating. *Ann N Y Acad Sci*, *1224*, 40-62. https://doi.org/10.1111/j.1749-6632.2011.05958.x

Little, S., Bonaiuto, J., Barnes, G., & Bestmann, S. (2019). Human motor cortical beta bursts relate to movement planning and response errors. *PLoS biology*, *17*(10), e3000479.

Lofredi, R., Tan, H., Neumann, W.-J., Yeh, C.-H., Schneider, G.-H., Kühn, A. A., & Brown, P. (2019). Beta bursts during continuous movements accompany the velocity decrement in Parkinson's disease patients. *Neurobiology of disease*, *127*, 462-471.

Love, J., Selker, R., Marsman, M., Jamil, T., Dropmann, D., Verhagen, J., Ly, A., Gronau, Q. F., Šmíra, M., & Epskamp, S. (2019). JASP: Graphical statistical software for common statistical designs. *Journal of Statistical Software*, *88*, 1-17.

Mars, R. B., Debener, S., Gladwin, T. E., Harrison, L. M., Haggard, P., Rothwell, J. C., & Bestmann, S. (2008). Trial-by-trial fluctuations in the event-related electroencephalogram reflect dynamic changes in the degree of surprise. *J Neurosci*, *28*(47), 12539-12545. https://doi.org/10.1523/JNEUROSCI.2925-08.2008

Muralidharan, V., Aron, A. R., & Schmidt, R. (2022). Transient beta modulates decision thresholds during human action-stopping. *Neuroimage*, *254*, 119145.

Nassar, M. R., Bruckner, R., & Frank, M. J. (2019). Statistical context dictates the relationship between feedback-related EEG signals and learning. *Elife*, *8*. https://doi.org/10.7554/eLife.46975

Novembre, G., Pawar, V. M., Bufacchi, R. J., Kilintari, M., Srinivasan, M., Rothwell, J. C., Haggard, P., & Iannetti, G. D. (2018). Saliency Detection as a Reactive Process: Unexpected Sensory Events Evoke Corticomuscular Coupling. *J Neurosci*, *38*(9), 2385-2397. https://doi.org/10.1523/JNEUROSCI.2474-17.2017

O'Reilly, J. X., Schuffelgen, U., Cuell, S. F., Behrens, T. E., Mars, R. B., & Rushworth, M. F. (2013). Dissociable effects of surprise and model update in parietal and anterior cingulate cortex. *Proc Natl Acad Sci U S A*, *110*(38), E3660-3669. https://doi.org/10.1073/pnas.1305373110

Parmentier, F. B., Elford, G., Escera, C., Andres, P., & San Miguel, I. (2008). The cognitive locus of distraction by acoustic novelty in the cross-modal oddball task. *Cognition*, *106*(1), 408-432. https://doi.org/10.1016/j.cognition.2007.03.008

Perrin, F., Pernier, J., Bertrand, O., & Echallier, J. F. (1989). Spherical splines for scalp potential and current density mapping. *Electroencephalogr Clin Neurophysiol*, *72*(2), 184-187. https://doi.org/10.1016/0013-4694(89)90180-6

Phillips, H. N., Blenkmann, A., Hughes, L. E., Kochen, S., Bekinschtein, T. A., Cam, C., & Rowe, J. B. (2016). Convergent evidence for hierarchical prediction networks from human electrocorticography and magnetoencephalography. *Cortex*, *82*, 192-205. https://doi.org/10.1016/j.cortex.2016.05.001

Pina-Fuentes, D., van Zijl, J. C., van Dijk, J. M. C., Little, S., Tinkhauser, G., Oterdoom, D. L. M., Tijssen, M. A. J., & Beudel, M. (2019). The characteristics of pallidal low-frequency and beta bursts could help implementing adaptive brain stimulation in the parkinsonian and dystonic internal globus pallidus. *Neurobiol Dis*, *121*, 47-57. https://doi.org/10.1016/j.nbd.2018.09.014

Raud, L., & Huster, R. J. (2017). The Temporal Dynamics of Response Inhibition and their Modulation by Cognitive Control. *Brain Topogr*, *30*(4), 486-501. https://doi.org/10.1007/s10548-017-0566-y

Raud, L., Huster, R. J., Ivry, R. B., Labruna, L., Messel, M. S., & Greenhouse, I. (2020). A Single Mechanism for Global and Selective Response Inhibition under the Influence of Motor Preparation. *J Neurosci*, *40*(41), 7921-7935. https://doi.org/10.1523/JNEUROSCI.0607-20.2020

Seer, C., Lange, F., Boos, M., Dengler, R., & Kopp, B. (2016). Prior probabilities modulate cortical surprise responses: A study of event-related potentials. *Brain Cogn*, *106*, 78-89. https://doi.org/10.1016/j.bandc.2016.04.011

Shannon, C. E. (1948). A mathematical theory of communication. *The Bell system technical journal*, *27*(3), 379-423.

Sherman, M. A., Lee, S., Law, R., Haegens, S., Thorn, C. A., Hämäläinen, M. S., Moore, C. I., & Jones, S. R. (2016). Neural mechanisms of transient neocortical beta rhythms: Converging evidence from

humans, computational modeling, monkeys, and mice. *Proceedings of the National Academy of Sciences*, *113*(33), E4885-E4894.

Shin, H., Law, R., Tsutsui, S., Moore, C. I., & Jones, S. R. (2017). The rate of transient beta frequency events predicts behavior across tasks and species. *Elife*, *6*. https://doi.org/10.7554/eLife.29086

Soh, C., Hynd, M., Rangel, B. O., & Wessel, J. R. (2021). Adjustments to Proactive Motor Inhibition without Effector-Specific Foreknowledge Are Reflected in a Bilateral Upregulation of Sensorimotor beta-Burst Rates. *J Cogn Neurosci*, 1-16. https://doi.org/10.1162/jocn_a_01682

Soh, C., & Wessel, J. R. (2021). Unexpected Sounds Nonselectively Inhibit Active Visual Stimulus Representations. *Cereb Cortex*, *31*(3), 1632-1646. https://doi.org/10.1093/cercor/bhaa315

Tatz, J. R., Soh, C., & Wessel, J. R. (2021). Common and Unique Inhibitory Control Signatures of Action-Stopping and Attentional Capture Suggest That Actions Are Stopped in Two Stages. *J Neurosci*, *41*(42), 8826-8838. https://doi.org/10.1523/JNEUROSCI.1105-21.2021

Tenke, C. E., & Kayser, J. (2005). Reference-free quantification of EEG spectra: combining current source density (CSD) and frequency principal components analysis (fPCA). *Clin Neurophysiol*, *116*(12), 2826-2846. https://doi.org/10.1016/j.clinph.2005.08.007

Tinkhauser, G., Pogosyan, A., Little, S., Beudel, M., Herz, D. M., Tan, H., & Brown, P. (2017). The modulatory effect of adaptive deep brain stimulation on beta bursts in Parkinson's disease. *Brain*, *140*(4), 1053-1067. https://doi.org/10.1093/brain/awx010

Tinkhauser, G., Pogosyan, A., Tan, H., Herz, D. M., Kuhn, A. A., & Brown, P. (2017). Beta burst dynamics in Parkinson's disease OFF and ON dopaminergic medication. *Brain*, *140*(11), 2968-2981. https://doi.org/10.1093/brain/awx252

Tinkhauser, G., Torrecillos, F., Duclos, Y., Tan, H., Pogosyan, A., Fischer, P., Carron, R., Welter, M. L., Karachi, C., Vandenberghe, W., Nuttin, B., Witjas, T., Regis, J., Azulay, J. P., Eusebio, A., & Brown, P. (2018). Beta burst coupling across the motor circuit in Parkinson's disease. *Neurobiol Dis*, *117*, 217-225. https://doi.org/10.1016/j.nbd.2018.06.007

Verbruggen, F., Aron, A. R., Band, G. P., Beste, C., Bissett, P. G., Brockett, A. T., Brown, J. W., Chamberlain, S. R., Chambers, C. D., Colonius, H., Colzato, L. S., Corneil, B. D., Coxon, J. P., Dupuis, A., Eagle, D. M., Garavan, H., Greenhouse, I., Heathcote, A., Huster, R. J., . . . Boehler, C. N. (2019). A consensus guide to capturing the ability to inhibit actions and impulsive behaviors in the stop-signal task. *Elife*, *8*. https://doi.org/10.7554/eLife.46323

Verbruggen, F., & Logan, G. D. (2009). Models of response inhibition in the stop-signal and stop-change paradigms. *Neuroscience & Biobehavioral Reviews*, *33*(5), 647-661.

Wessel, J. R. (2018a). A Neural Mechanism for Surprise-related Interruptions of Visuospatial Working Memory. *Cereb Cortex*, *28*(1), 199-212. https://doi.org/10.1093/cercor/bhw367

Wessel, J. R. (2018b). Surprise: A More Realistic Framework for Studying Action Stopping? *Trends Cogn Sci*, *22*(9), 741-744. https://doi.org/10.1016/j.tics.2018.06.005

Wessel, J. R. (2020). beta-Bursts Reveal the Trial-to-Trial Dynamics of Movement Initiation and Cancellation. *J Neurosci*, *40*(2), 411-423. https://doi.org/10.1523/JNEUROSCI.1887-19.2019

Wessel, J. R., & Aron, A. R. (2013). Unexpected events induce motor slowing via a brain mechanism for action-stopping with global suppressive effects. *J Neurosci*, *33*(47), 18481-18491. https://doi.org/10.1523/JNEUROSCI.3456-13.2013

Wessel, J. R., & Aron, A. R. (2015). It's not too late: the onset of the frontocentral P3 indexes successful response inhibition in the stop-signal paradigm. *Psychophysiology*, *52*(4), 472-480. https://doi.org/10.1111/psyp.12374

Wessel, J. R., & Aron, A. R. (2017). On the Globality of Motor Suppression: Unexpected Events and Their Influence on Behavior and Cognition. *Neuron*, *93*(2), 259-280. https://doi.org/10.1016/j.neuron.2016.12.013

Wessel, J. R., & Huber, D. E. (2019). Frontal cortex tracks surprise separately for different sensory modalities but engages a common inhibitory control mechanism. *PLoS Comput Biol*, *15*(7), e1006927. https://doi.org/10.1371/journal.pcbi.1006927

Wessel, J. R., Reynoso, H. S., & Aron, A. R. (2013). Saccade suppression exerts global effects on the motor system. *J Neurophysiol*, *110*(4), 883-890. https://doi.org/10.1152/jn.00229.2013

Wessel, J. R., & Ullsperger, M. (2011). Selection of independent components representing event-related brain potentials: a data-driven approach for greater objectivity. *Neuroimage*, *54*(3), 2105-2115.

APPENDIX

As a subsidiary goal of this study, we sought to identify whether the EEG data in Dataset 1 replicated the whole-brain event-related EEG findings reported by Wessel and Huber (2019), especially since their data were re-analyzed as Dataset 2. We also aimed to extend their findings to unexpected events originating from the haptic modality. In general, the results closely followed those of Wessel and Huber (2019) further underscoring the similarity of Datasets 1 and 2, despite the inclusion of the third haptic modality in Dataset 1.

EEG analyses following Wessel and Huber (2019). We considered four results from Wessel and Huber (2019) to be of primary importance in replicating their work:

1) single-trial EEG data should favor a model with separate Bayesian surprise terms in all three modalities (auditory, visual, and haptic)

2) mean RT should be predicted by FC P3 in each modality

3) the FC P3 following unexpected events should be recoverable from a FC IC isolated from the stop-signal task when used as a functional localizer (i.e., the stop-related FC P3)

4) the separate Bayesian surprise model should be implicated with this IC alone

Given that we examined β-bursts for both Shannon and Bayesian surprise, for the sake of thoroughness, we also newly examined the abovementioned analyses in Dataset 2 based on Shannon surprise. The ensuing description of the methods relevant to this subsection is adapted from Wessel and Huber (2019):

First, the surprise values originating from both types of surprise (Shannon, Bayesian surprise) and modality considerations (separate, combined) were used to model the whole-brain event-related single-trial EEG response on trials with unexpected events. We based this analysis on procedures reported by Fischer and Ullsperger (2013). To compare surprise models, at the

single-trial level, we used robust regression [in MATLAB, robustfit()] to fit the standardized (*z*-scored) EEG signal with the standardized (*z*-scored) surprise values in each participant in each electrode in each trial in 48 ms time windows spanning from 50 to 500 ms. These data were baseline corrected with the data from -100 to 0 ms and averaged across trials (48 trials, barring those excluded because of artifacts). For each model specification, this resulted in a 64 (channel) * 10 (time point) = 640 matrix of beta weights. At the group level, the mean beta weights corresponding to the models were tested against 0 (using one-sample *t*-tests) and separate and combined models were tested against each other (using paired-samples *t*-tests) within each type of surprise. Multiple comparisons were corrected for three sets of 640 *t*-tests via a false discovery rate correction (FDR-corrected, $p < .01$) procedure (FDR, Benjamini et al., 2006).

Second, we examined Bayesian Pearson correlations between the mean amplitudes of the P3 responses following each type of unexpected event (auditory, visual, and haptic) and the corresponding mean RT. The subject-average amplitudes were determined by finding the largest positive-going amplitude deflection in the trial-average (at electrodes FCz and Cz) during the time-window ranging from 150-500 ms after the unexpected event (or in the case of the visual P3, we modified this search range to 250-600 ms based on the characteristics of the response reported in Wessel and Huber).

Third, the SST was employed as a functional localizer to demonstrate that the surprise-related FC P3 response shares a common neural generator with the inhibition related FC P3 response in the SST. To this end, the two datasets from the CMO and SST task were merged, and the preprocessing steps and the ICA detailed above were repeated anew on the merged datasets. The stop-related P3 IC was selected automatically using a two-step spatiotemporal selection procedure (Wessel & Ullsperger, 2011). First, components were identified whose back-projected

channel-space topography showed a maximum positive difference in stop compared to go trials in a FC ROI (consisting of electrodes FC1, FCz, FC2, C1, Cz, and C2 from among 9 ROIs across the scalp). From these components, the component that showed the highest correlation to the original channel-space ERP in the same FC ROI and time window was selected for each participant as their stop-related IC. In Dataset 1, we validated the IC selected stop-signal P3 using a two-fold procedure that addresses whether the stop-signal P3 occurs earlier on successful stops and whether its onset is positively correlated with SSRT. In short, we replicated prior work using this validation procedure (Kok et al., 2004; Wessel & Aron, 2015; Wessel & Huber, 2019). We do not report these results here (but refer the interested reader to the data and code on OSF).

Fourth, we repeated the surprise model analyses detailed in (1) using only each subject's selected Stop-related IC for the unexpected event in the CMO task. As control analyses, we subjected two other versions of the merged dataset to the same analyses. These included reconstructions of the channel-space based on a back-projection of all original ICs *sans* the Stop-related IC and a back-projection of the IC that accounted for the most residual variance after the Stop-related IC was removed. As in (1), these tests were FDR-corrected for multiple comparisons (which again included 640 tests per set).

Replication of Wessel and Huber (2019) and extension to haptic domain. We now report on the four results that we considered to be of primary importance (as detailed in the corresponding portion of the Method section) to replicate Wessel and Huber (2019) and extend their findings to the haptic domain:

First, using Dataset 1, we aimed to replicate Wessel and Huber's (2019) finding involving Bayesian surprise that a model with separate surprise terms for each modality would better explain the single-trial EEG response than the combined data and that the spatiotemporal dynamics of any

significant time periods would relate to those of the P3 response. These tests were FDR-corrected for a family-wise alpha-level of .01. As can be seen in Fig. A1, the separate surprise term model showed a significant, positive prediction of the EEG data beginning with the 326-374 ms bin and extending through the remaining time bins (i.e., to 476-524 ms) to around the onset of the imperative stimulus. For the combined surprise term model, the 276-324 ms bin showed a significant positive prediction of the EEG data which also extended through the end of the trial. However, the separate surprise term model fit the data better than the combined surprise term model beginning with the 326-374 ms bin and onwards. The difference between the one earlier bin (276-324 ms) in the combined surprise term model with the corresponding portion in the separate surprise term model was not significant. Compared to Wessel and Huber, the bin in which we first observed the separate surprise term model was slightly later (326-374 ms compared to 276-324 ms). This might be attributable to the larger sample size in Dataset 2 or the inclusion of unexpected events in the haptic modality in Dataset 1. Nevertheless, this time range coincided with the FC P3 response within each modality. In addition, the mean standardized beta-weights at model-fitting electrodes identified by Wessel and Huber (FC2, C1, Cz, and C2) were all reliably above zero when fitting the Bayesian surprise model with separate modality terms. We therefore replicated Wessel and Huber with the current, trimodal dataset in showing that a model with separate surprise terms (involving Bayesian surprise) predicts the single-trial EEG data.

A Bayesian surprise

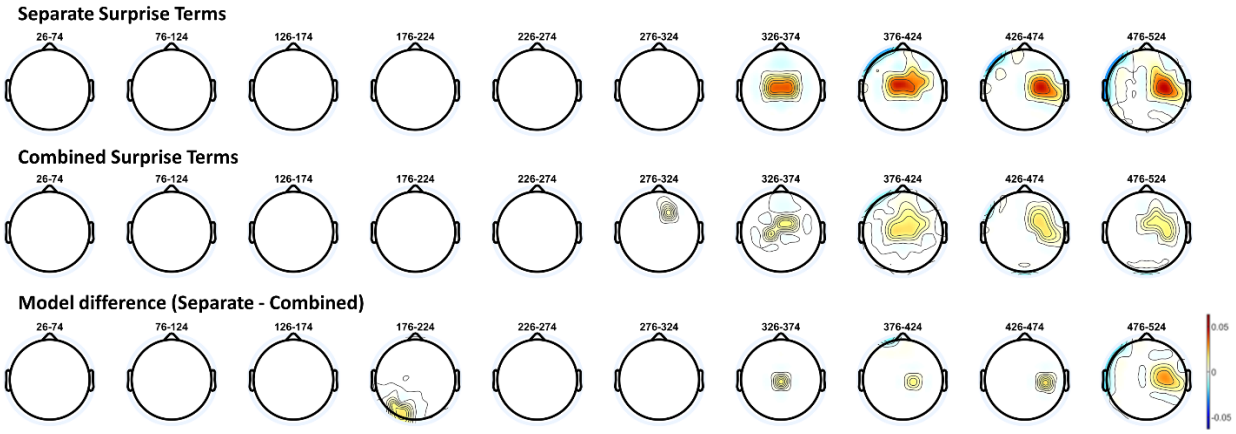

B Shannon surprise

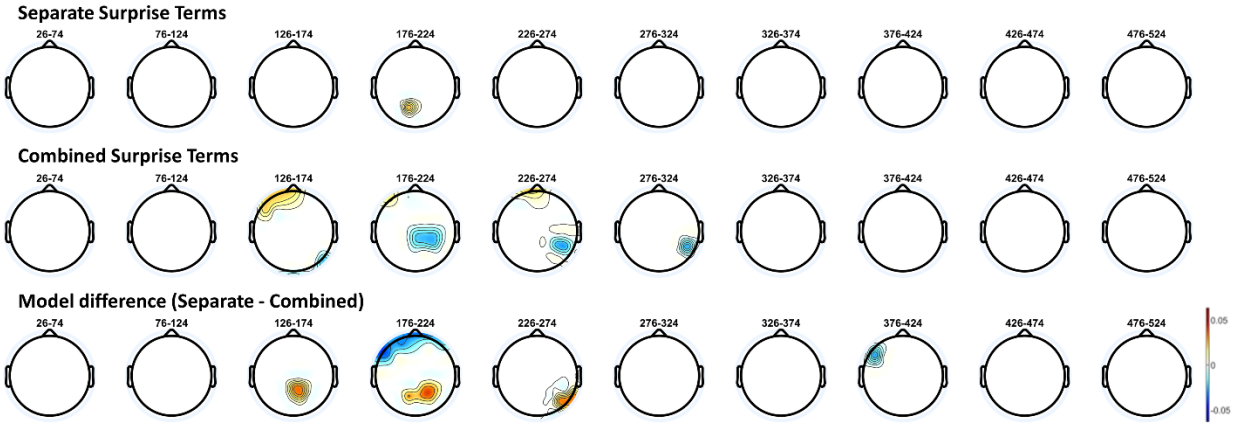

C ERP at model-fitting electrodes

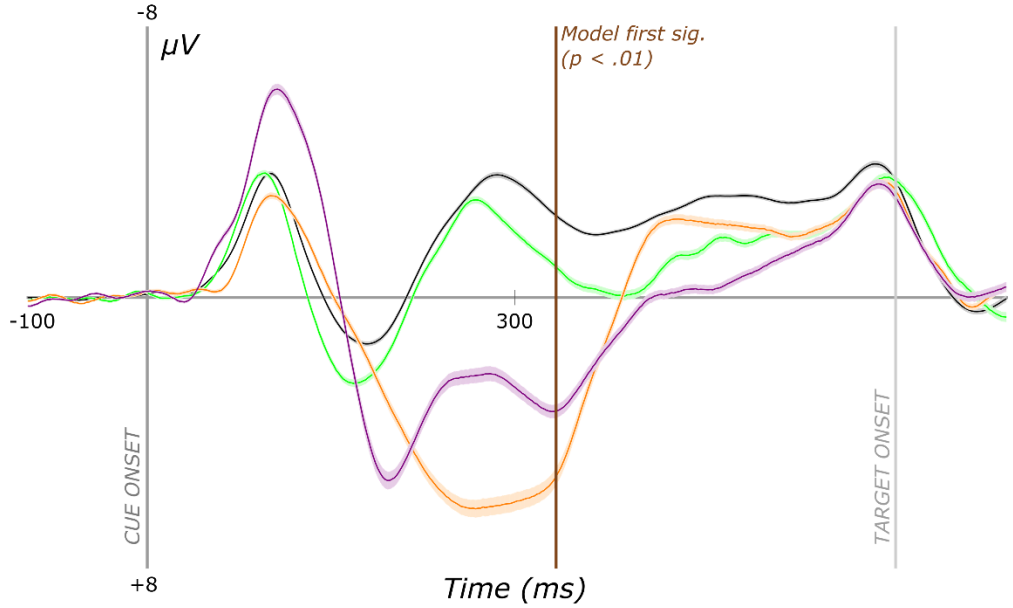

Fig. A1. Scalp-topographies from modeling whole-brain single-trial EEG data with surprise and event-related potential at model-fitting electrodes in Dataset 1. a *Topographies represent the mean standardized individual beta weights for Bayesian surprise and separate modality terms (top row), Bayesian surprise and combined modality terms (mid row), and the difference in fits between these two models (bot row). Heatmaps reflect beta weights.* ***b*** *The same analyses as panel a but with Shannon surprise terms.* ***c*** *Cue-locked event-related potentials following each event type at model-fitting electrodes (FC2, C1, Cz, and C2) that were significant for the winning Bayesian surprise model and in Dataset 2. The spatiotemporal dynamics of the model-fitting electrodes correspond to the FC P3.*

Given that we examined β-bursts with respect to Shannon surprise (in addition to Bayesian surprise), we repeated the above analyses using Shannon surprise and with both datasets (since Wessel and Huber had not examined this for Dataset 2). For Dataset 1 (see Fig. A1b), Shannon surprise fitted the whole-brain EEG data at some electrode sites (both positively and negatively), but rather inconsistently and not at FC sites. For Dataset 2, however, Shannon surprise significantly fit the data in the 326-374 ms time bin and at FC sites. Significant model fits were not found with common surprise terms and no differences between model fits were found, either.

Second, we correlated the mean amplitude of the FC P3 response in each modality with mean RT (see Fig. A2). Reliable, medium-sized positive correlations were found between RT and P3 amplitude following unexpected events in each modality, including the new haptic modality (unexpected visual: $r = .41$, $BF_{10} = 10.78$; unexpected audio: $r = .38$, $BF_{10} = 5.87$; unexpected haptic: $r = .39$, $BF_{10} = 7.63$). This is consistent with Wessel and Huber's findings in the auditory

and visual modalities and further links this functional signature to inhibition (as larger responses brought about slower RT).

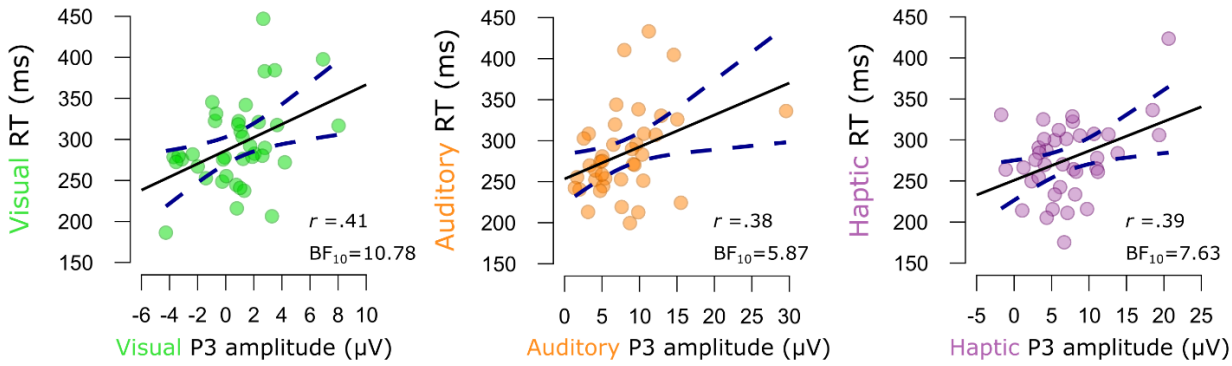

Fig. A2. Pearson correlations between mean FC P3 amplitude and mean RTs following each type of unexpected event in Dataset 1. *Dots indicate the means from individual subjects. Solid black lines indicate the slope of the linear model. Dotted dark blue lines indicate the ±95 % confidence intervals.*

Third, having merged the datasets from the visual SST and CMO tasks and having isolated a frontocentral stop-related IC from each subject, we aimed to recover the FC P3 response using this one independent component. Since ICA serves to unmix a signal into its constituent (orthogonal) sources, identifying the FC P3 in the CMO task by using the SST as a functional localizer would suggest that a common neural generator is responsible for the FC P3 in both contexts. Since the SST was completed only in the visual modality, identification of FC P3 in the other auditory and haptic modalities would further highlight this signature as a domain-general inhibitory signature—granted, one that still retains information about the sensory modalities prompting inhibition (otherwise, the surprise model fitting results would have favored the common

surprise term model). The difference waves are shown in Fig. 8 in the main text. We were indeed able to produce the FC P3 in the CMO task when using the SST as a functional localizer task.

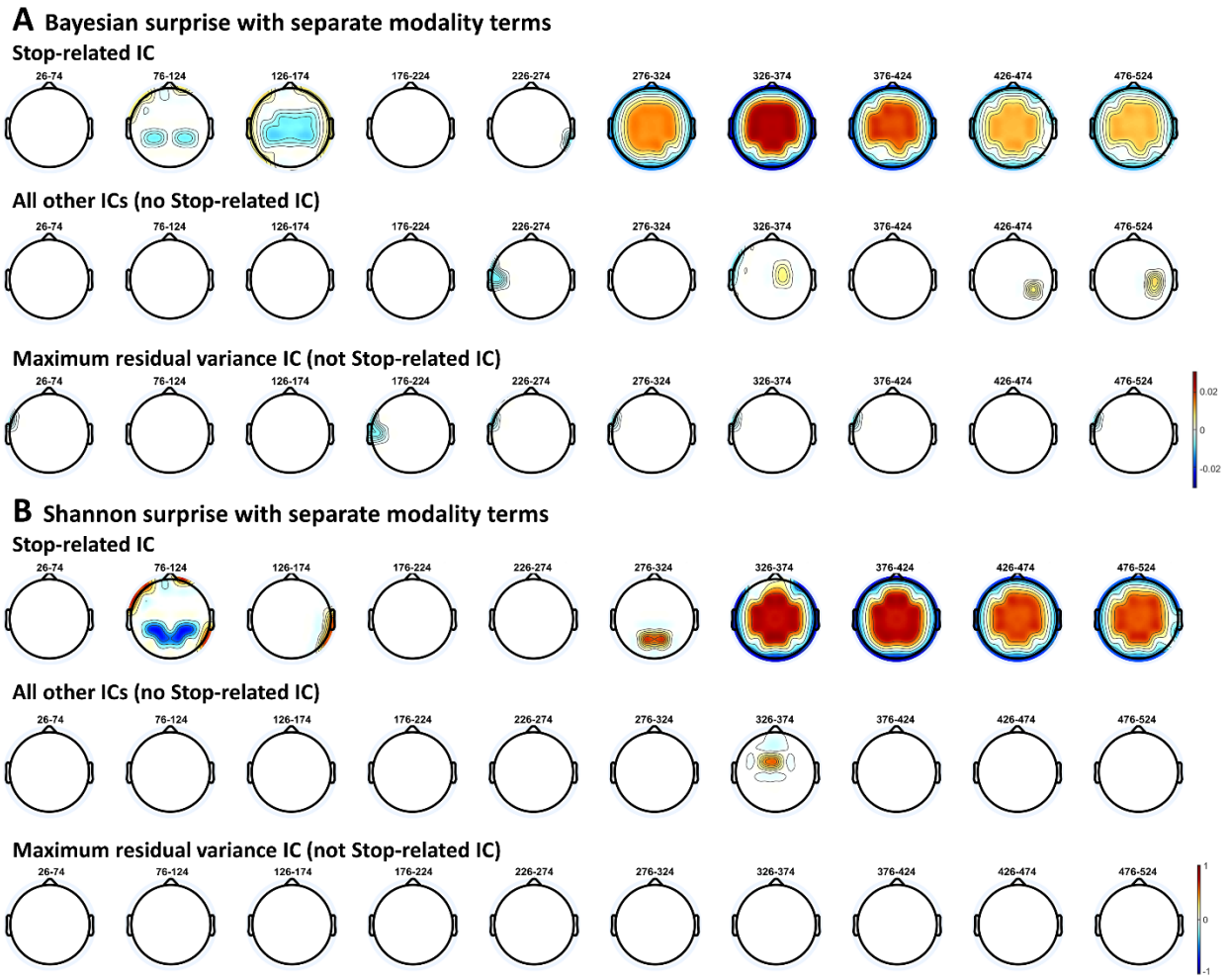

Fig. A3. Scalp-topographies of the ICs modeled with Bayesian surprise and Shannon surprise in the CMO task of Dataset 1 (n=39). a *Beta-weights from the single-trial model-fitting of IC-EEG data with Bayesian surprise under the winning separate modality term model. Colors indicate significant model fits (warm colors = positive, cool colors = negative; white = non-significant, p = .01, FDR-corrected).* ***b*** *The same analyses but with Shannon surprise.*

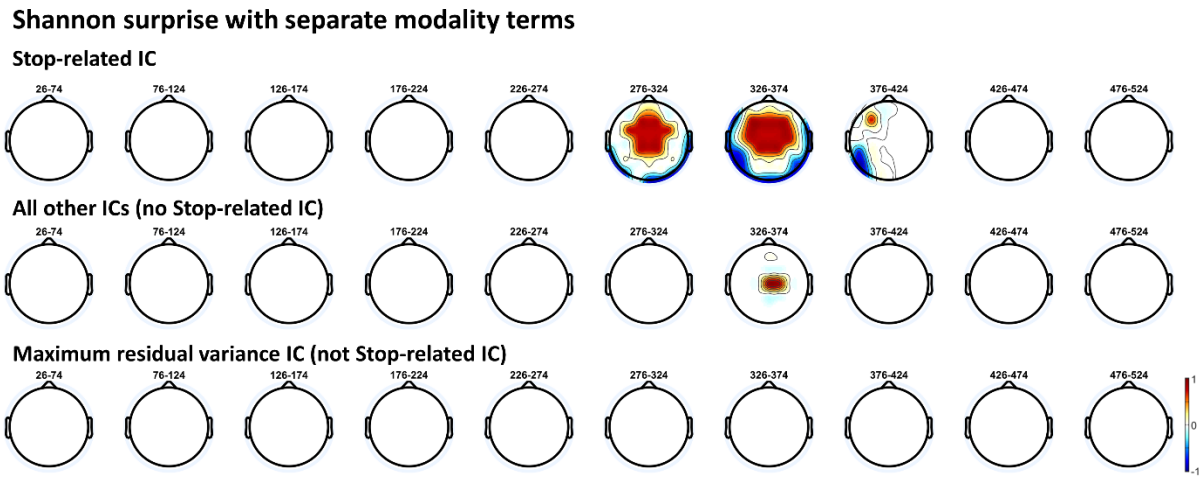

Fig. A4. Scalp-topographies of the ICs modeled with Shannon surprise in the CMO task of Dataset 2 (n=55). *The same as Fig. A3b but with Dataset 2.*

As our final replication of Wessel and Huber with Dataset 1, we repeated the abovementioned whole-brain, single-trial EEG response modeling with surprise, this time using only the Stop-related IC. For control analyses, we also completed these analyses using all other ICs and the IC that explained the most variance upon removal of the stop-related IC. As can be seen in Fig. A3*a*, Bayesian surprise clearly fit the stop-related IC in Dataset 1. Moreover, this occurred at FC sites and timepoints consistent with the FC P3, suggesting that the neural generator involved in action inhibition in the SST also tracked surprise within the context of the CMO task. Interestingly, with the stop-related IC, Shannon surprise also fit the data at these same electrode sites and timepoints. This contrasts the model-fitting analysis involving the full EEG data which did not bear these relationships (see Fig. A1). Dataset 2 also replicated this finding of positive relationships between Shannon surprise and stop-related IC activity at FC sites. Here, significant model fits were found in the 276-324 and 326-374 ms bins. Most basically, the results from the IC-based approach replicate Dataset 2 in suggesting that the FC P3 process involved in action

stopping also tracks surprise within the context of a CMO task. We further show here that using the IC-based approach, Shannon surprise also predicts activity at FC sites around the time of the FC P3 in Dataset 2 (see Fig. A4). This could simply be because our experimental designs did not attempt to decorrelate Bayesian surprise and Shannon surprise. Future work might attempt to do so by intentionally introducing long stretches of intervening standard events between the same type of unexpected events to see if FC P3 is better captured by Bayesian surprise and whether another IC relating to the centro-parietal P3 better captures Shannon surprise (e.g., Mars et al., 2008; Seer et al., 2016).